Utah State University
DigitalCommons@USU

All Graduate Theses and Dissertations | Graduate Studies

5-1997

Evaluation of Two-Dimensional Hydraulic Modeling in a Natural River and Implications in Instream Flow Assessment Methods

Karl L. Tarbet
Utah State University

Follow this and additional works at: https://digitalcommons.usu.edu/etd

Part of the Civil and Environmental Engineering Commons

Recommended Citation

Tarbet, Karl L., "Evaluation of Two-Dimensional Hydraulic Modeling in a Natural River and Implications in Instream Flow Assessment Methods" (1997). *All Graduate Theses and Dissertations*. 4423.
https://digitalcommons.usu.edu/etd/4423

This Thesis is brought to you for free and open access by the Graduate Studies at DigitalCommons@USU. It has been accepted for inclusion in All Graduate Theses and Dissertations by an authorized administrator of DigitalCommons@USU. For more information, please contact digitalcommons@usu.edu.

UtahStateUniversity
MERRILL-CAZIER LIBRARY

EVALUATION OF TWO-DIMENSIONAL HYDRAULIC MODELING IN A NATURAL RIVER AND IMPLICATIONS IN INSTREAM FLOW ASSESSMENT METHODS

by

Karl L. Tarbet

A thesis submitted in partial fulfillment
of the requirements for the degree

of

MASTER OF SCIENCE

in

Civil and Environmental Engineering

UTAH STATE UNIVERSITY
Logan, Utah

1997

Copyright © Karl Tarbet 1997

All Rights Reserved

ABSTRACT

Evaluation of Two-Dimensional Hydraulic Modeling

in a Natural River and Implications in Instream

Flow Assessment Methods

by

Karl L. Tarbet, Master of Science

Utah State University, 1997

Major Professor: Dr. Thomas B. Hardy
Department: Civil and Environmental Engineering

The Logan River was used as a study site to assess the capabilities of two-dimensional depth-averaged hydraulic modeling in the x-y plane of a natural river for use with instream flow studies. Data were collected to spatially represent the study reach with depth, velocity, northing, easting, elevation, and substrate values using a total station and electronic velocity meter. Computational finite element meshes were generated using four different density levels of geometry data to examine the relationship between field data density and computational mesh on geometry errors. Geometry errors were found to be related to smoothing effects, which removed complex channel geometries while overall mesh geometry errors were related to data density in homogeneous versus heterogeneous channel conditions.

Results indicate that required field data can be optimized with lower data densities in homogenous sections of the river channel. Of the two hydraulic models examined, the U.S. Army Corps of Engineers RMA2 model could not be adequately calibrated given the high slope within the study reach and therefore all subsequent evaluations were made utilizing the CDG2D model. CDG2D model performance was best in the lower gradient sections of the test section at both calibrated and simulated flows with increasing errors for water surface and associated depth and velocity errors as channel gradient increased. These results suggest that additional research is needed to define limiting gradients under which application of this class of hydrodynamic model can be expected for practical instream flow assessments.

(89 pages)

ACKNOWLEDGMENTS

Funding for this research was provided in part by the United States Fish and Wildlife Service National Biological Survey, the Vice President of Research at Utah State University, and the Utah Water Research Laboratory.

I am thankful for the support and constant encouragement from Dr. Thomas Hardy. Without the support of my peer graduate students who are my friends, this project could not have been completed. Jennifer Ludlow and Nathan Bartsch especially helped collect data from the Logan River. I also thank Peter Steffler for his willingness to continually answer questions about the hydraulic modeling.

Karl L. Tarbet

CONTENTS

Page

ABSTRACT iii

ACKNOWLEDGMENTS v

LIST OF TABLES viii

LIST OF FIGURES ix

INTRODUCTION 1

MATERIALS AND METHODS 3

Site Description 3
Data Collection 3
Finite Element Hydraulic Modeling 4

RMA2 model 5
CDG2D model 6

Mesh Generation 8

FASTTABS 8
CDGMesh 15

Derivation of Computational Meshes 18
Calibration 18

Calibration of RMA2 20
Calibration of CDG2D 20

Calculation of Modeling Errors 22

RESULTS AND DISCUSSION 24

Geometry Errors 24
Water Surface Elevations at the Calibration Flows 27
Depth and Velocity Errors at the Calibration Flows 34
Comparison of Measured versus Predicted
Errors at Simulated Discharges 43

Water surface elevation errors 43
Depth and velocity errors 43

Hydraulic Modeling and Calibration 56

Influence of data collection and roughness assignment on calibration and modeling 56
Influence of mesh design on calibration and modeling 56
Influence of turbulence on calibration and modeling 58

Implications to Instream Flow Assessments 59

RECOMMENDATIONS 60

ENGINEERING SIGNIFICANCE 62

REFERENCES 64

APPENDIX 66

LIST OF TABLES

Table		Page
1	Geometry errors (feet) and density statistics	26
2	Velocity and depth errors at calibrations of 155 cfs and 255 cfs	36
3	Velocity and depth errors at simulations of 155 cfs and 255 cfs	49

LIST OF FIGURES

Figure		Page
1	Site location	4
2	Location of field sampling data based on 749 measurements within the Logan River	10
3	Location of field sampling data based on 575 measurements within the Logan River	11
4	Location of field sampling data based on 415 measurements within the Logan River	12
5	Location of field sampling data based on 283 measurements within the Logan River	13
6	Simple mesh	14
7	Relaxed simple mesh	14
8	Mesh smoothing error	15
9	Triangulation of raw field data	16
10	FASTTABS relaxed mesh	17
11	CDGMesh relaxed mesh	17
12	Computational mesh	19
13	Unstable solution of RMA2 water surface prediction	21
14	Mesh geometry errors as a function of the number of computational nodes	25
15	Geometry errors for different levels of field data	25
16	Spatial geometry errors for the 155 cfs data set	28
17	Spatial geometry errors for the 255 cfs data set (downstream)	29

18 Spatial geometry errors for the 255 cfs data set (upstream) 30

19 Water surface at the 155 cfs calibration 31

20 Water surface at the 255 cfs calibration (downstream) 32

21 Water surface at the 255 cfs calibration (upstream) 33

22 Depth errors at the 155 cfs calibration 35

23 Velocity errors at the 155 cfs calibration 35

24 Spatial depth errors at the 155 cfs calibration 37

25 Spatial velocity errors at the 155 cfs calibration 38

26 Spatial depth errors at the 255 cfs calibration (downstream) 39

27 Spatial depth errors at the 255 cfs calibration (upstream) 40

28 Spatial velocity errors at the 255 cfs calibration (downstream) 41

29 Spatial velocity errors at the 255 cfs calibration (upstream) 42

30 Water surface at the 155 cfs simulation 44

31 Water surface at the 255 cfs simulation (downstream) 45

32 Water surface at the 255 cfs simulation (upstream) 46

33 Depth errors at the 155 cfs simulation and calibration 47

34 Depth errors at the 255 cfs simulation and calibration 47

35 Velocity errors at the 155 cfs simulation and calibration 48

36 Velocity errors at the 255 cfs simulation and calibration 48

37 Spatial depth errors at the 155 cfs simulation 50

38 Spatial velocity errors at the 155 cfs simulation 51

39 Spatial depth errors at the 255 cfs simulation (downstream) 52

40 Spatial depth errors at the 255 cfs simulation (upstream) 53

41 Spatial velocity errors at the 255 cfs simulation (downstream) 54

42 Spatial velocity errors at the 255 cfs simulation (upstream) 55

INTRODUCTION

The most used, accepted, and debated instream flow assessment tool is the Instream Flow Incremental Methodology (IFIM) (Orth and Maughan, 1982; Mathur et al., 1985; Shirvell, 1986; Scott and Shirvell, 1987; Reiser, Wesche, and Estes 1989). Aside from this debate, an integral part of the IFIM is a set of hydraulic and habitat models referred to as the Physical Habitat Simulation System (PHABSIM) and is utilized to evaluate the quantity and quality of fisheries habitat as a function of discharge (Milhous, Updike, and Schneider, 1989; Bovee, 1995). A central feature of PHABSIM is the use of a variety of one-dimensional hydraulic simulation routines that rely on cross-section data of the river geometry, water surface elevations at different discharges, and observed velocities to calibrate these models. The calibrated hydraulic models are then utilized to simulate the hydraulic attributes of depth and velocity over a user specified range of discharges. However, the application of the one-dimensional hydraulic models in PHABSIM obtains a simplified picture of the actual hydraulics, which is not always considered sufficient (Ghanem and Hicks, 1992). In particular, PHABSIM calculates velocities at a cross section by dividing the river into independent cells and then solves Manning's equation in terms of velocity for each cell for a specified discharge. The calibrated Manning's n value at each cell (or vertical) is most often determined from a single set of measured velocities across each cross section. When modeling a river with cross sections that may be anywhere from 10 meters to many hundreds of meters apart, detailed velocity information throughout the spatial domain within the channel cannot be obtained. Although selecting a large number of cross sections over very small areas (i.e., a

few meters) will likely improve velocity prediction capabilities, use of one-dimensional hydraulics is still limited in its ability to accurately predict flow about complex channel geometries that have significant two and three-dimensional characteristics. Additionally, the cost and time constraints in operational instream flow studies typically preclude collection of cross sections at this level of measurement scale. Recently, because of the advances in the capabilities of computers and spatial sampling technologies, models for two-dimensional hydraulics are becoming more widely available and application of two-dimensional hydraulics within the area of instream flow assessments is now occurring (Leclerc et al., 1995). However, the benefits of these models need to be addressed in terms of the data requirements and an estimation of anticipated hydraulic simulation errors within natural channels needs to be compared to applications using more traditional one-dimensional hydraulics.

The purpose of this thesis is to communicate the results from field testing two-dimensional hydraulic models. Research will be presented in three parts: first, determine the accuracy of spatially predicting depths and velocities at specific calibration flow rates; second, explore the influence of data collection density on these predictions, and third, measure the ability of two-dimensional models to predict depth and velocities at simulated flows other than the calibration flow.

MATERIAL AND METHODS

Site Description

A 1600-foot reach within the Logan River in northeastern Utah, USA, was chosen for study (Figure 1). The reach starts 100 feet below First Dam, upstream of the Utah State University Water Research Lab (UWRL), and continues downstream for approximately 1600 feet below the dam. The width of the Logan River throughout the reach ranged from approximately 20 to 60 feet and has an average gradient of 1.0 percent and a maximum gradient of 2.5 percent. The majority of the substrate is made up of cobble and boulder with some small areas of gravel. The study reach has four classes of habitat: run (57 percent), riffle (14 percent), turbulent (16 percent), and pool (13 percent). The three dominant species of fish include mountain whitefish (*Prosopium williamsoni*), albino rainbow trout (*Oncorhynchus mykiss*), and brown trout (*Salmo trutta*).

Data Collection

Field data were collected along 1600 feet of the Logan River during the summer and fall of 1995. Channel geometry data were collected roughly in the manner outlined by Ghanem (1995), such that the river can be represented by a finite element mesh, which interpolates geometry between collection points. Sampling occurred throughout the river using an irregular systematic point sampling procedure where channel geometry varied substantially between cross sections. At each spatial domain data point, bed elevation, mean column velocity, depth, and substrate characteristics were recorded. These

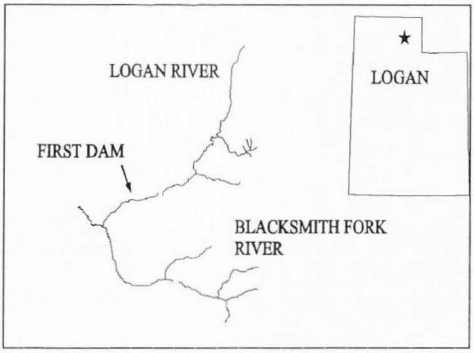

Figure 1. Site location.

measurements were made with spatial overlap for different flow rates as the flows decreased from 272 cfs at the end of July to 120 cfs in October. A Topcon GTS-300 total station with attached data logger was used to collect the geometry as northing, easting, and elevation. A Swoffer velocity meter with attached wading rod was used to collect depths and velocites. Velocites were recorded at six tenths of the total depth measured from the surface down as a twenty-second average. This data is listed in Appendix A.

Finite Element Hydraulic Modeling

The Logan River was modeled with the U.S. Army Corps of Engineers two-dimensional finite element model RMA2 and also modeled with CDG2D developed by the University of Edmonton in Alberta, Canada (Ghanem, 1995). RMA2 and CDG2D both solve simplified forms of the three-dimensional Reynolds form of the Navier-Stokes

equations by integration of the equations over the depth, resulting in two-dimensional equations. This simplification limits the velocity calculations to the horizontal plane such that the velocities are averaged over the depth of flow.

RMA2 model

The basic form of the RMA2 model is given as:

$$\frac{\partial u}{\partial t} + u\frac{\partial u}{\partial x} + v\frac{\partial u}{\partial y} + g\frac{\partial h}{\partial x} + g\frac{\partial a}{\partial x} - \frac{\varepsilon_{xx}}{\rho}\frac{\partial^2 u}{\partial x^2} - \frac{\varepsilon_{xy}}{\rho}\frac{\partial^2 u}{\partial y^2} + \frac{gu}{C^2 h}\sqrt{u^2 + v^2} = 0$$

$$\frac{\partial v}{\partial t} + u\frac{\partial v}{\partial x} + v\frac{\partial v}{\partial y} + g\frac{\partial h}{\partial y} + g\frac{\partial a}{\partial y} - \frac{\varepsilon_{yx}}{\rho}\frac{\partial^2 v}{\partial x^2} - \frac{\varepsilon_{yy}}{\rho}\frac{\partial^2 v}{\partial y^2} + \frac{gv}{C^2 h}\sqrt{u^2 + v^2} = 0$$

$$C = \frac{h^{\frac{1}{6}}}{n}$$

$$\frac{\partial h}{\partial t} + h\left(\frac{\partial u}{\partial x} + \frac{\partial v}{\partial y}\right) + u\frac{\partial h}{\partial x} + v\frac{\partial h}{\partial y} = 0$$

where:

u,v = x and y components of velocity

g = Acceleration due to gravity

h = Depth

a = Elevation of bottom

ε_{xx} ε_{xy} ε_{yx} ε_{yy} = eddy viscosity coefficients

ρ = Density of water

n = Manning's roughness value

Turbulence is modeled using the eddy viscosity coefficients. The finite element formulation uses the Galerkin method of weighted residuals. Triangular six-node elements were used which have quadratic shape functions for velocity and linear shape functions for depth. All solutions were obtained for steady-state conditions using the Newton-Raphson iteration method. RMA2 models subcritical flow only. RMA2 is formulated in terms of velocity instead of unit discharge since this improved the algorithm solution behavior (Boss International, 1993).

Boundary conditions were specified using a series of nodes to define the upstream flow line and another series of nodes to define the downstream water surface elevation line. The water surface elevation line specifies all nodes along that line that have a constant specified water surface elevation. The flow line defines a flow rate and the direction flow enters the upstream boundary. Within this study, the direction of flow was set to be perpendicular to the axis of the upstream channel geometry. Simulations were started with a constant initial water surface elevation slightly higher than the highest geometry elevation specified for the entire computational mesh. A downstream water surface elevation slightly lower than the initial water surface was specified.

CDG2D model

The CDG2D Finite Element model is also based on the Reynolds form of the Navier-Stokes equations and uses the Chezy coefficient based on relative roughness to model bottom friction based on the equations for steady one-dimensional flow. This model uses modified weighting functions in the finite element formulation to achieve up-winding effects for increased model stability in the iteration solution process. The

CDG2D model supports unsteady flow, both super and subcritical flows, with the ability to simulate dry regions. The basic form of the CDG2D model is given as:

$$\frac{\partial H}{\partial t}+\frac{\partial q_x}{\partial x}+\frac{\partial q_y}{\partial y}=0$$

$$\frac{\partial q_x}{\partial t}+\frac{\partial}{\partial x}(U q_x)+\frac{\partial}{\partial y}(V q_x)+\frac{g}{2}(\frac{\partial}{\partial x}(H^2))=gH(S_{ox}-\frac{U\sqrt{U^2+V^2}}{C_s^2 gH})+\frac{1}{\rho}(\frac{\partial}{\partial x}(H\tau_{xx}))$$

$$\frac{\partial q_y}{\partial t}+\frac{\partial}{\partial x}(U q_y)+\frac{\partial}{\partial y}(V q_y)+\frac{g}{2}(\frac{\partial}{\partial y}(H^2))=gH(S_{oy}-\frac{V\sqrt{U^2+V^2}}{C_s^2 gH})+\frac{1}{\rho}(\frac{\partial}{\partial y}(H\tau_{yy}))$$

$$C_s=6.2+5.75\log(\frac{H}{k_s})$$

where:

H = Depth

q_x, q_x = discharge per unit width

U, V = x- and y- components of velocity

S_{ox}, S_{oy} = bed slope components

k_s = bed roughness height

Boundary conditions were specified using flow boundaries at the edges of the upstream domain of the mesh and water-surface elevations at the downstream boundary of the mesh similar to RMA2. The flow boundary defines a series of edges where flow enters the mesh. The water-surface elevation boundary defines a constant water surface at the

downstream edge of the mesh. The CDG2D model also requires that all exterior edges be numbered in sequence; then both water-surface boundaries and flow boundaries were defined by the beginning and ending boundary segment numbers. FASTTABS-generated meshes were used with the CDG2D model by developing a translation program that converts FASTTABS geometry files into CDG2D input files. Initial water surface elevations were computed by developing another program, ASSIGNIC, which assigns a given estimated water surface profile to the CDG2D input file. The CDG2D model was run until steady-state conditions were achieved. A recommended value of twice the average travel time for the modeled reach was used as a guide in reaching steady state (Steffler, personal communication, 1997).

Mesh Generation

Meshes were constructed with both FASTTABS and CDGMesh. Both software packages are useful tools and a combination of these packages worked best for creating meshes of the Logan River, suitable for use with both the RMA2 and CDG2D hydraulic models. FASTTABS was used to construct unstructured meshes that represent the spatial geometry and CDGMesh was used to construct more structured computational meshes, using the nodes from the FASTTABS-generated mesh to compute nodal elevations in the computational mesh.

FASTTABS

FASTTABS software (Boss International, 1993) simplifies mesh design by automatically generating triangulating irregular networks (TIN) based on linear three node

elements using raw data. FASTTABS was used to visualize field data and interpolate additional points along the longitudinal direction of the stream as needed to best represent the geometry of the river. A utility was developed to convert FASTTABS meshes into a format usable by the CDG2D hydraulic model. By using FASTTABS, four sets of data were generated that represent the bed topography of the Logan River at different densities of field data. Figures 2-5 contain 749, 575, 415, and 283 points, respectively.

FASTTABS smoothes elements by moving nodes of elements to the centroid of the surrounding elements by changing the x and y coordinates, giving elements a more uniform shape. For example, consider the simple mesh in Figure 6. The z coordinate at the new (x,y) position (Figure 7) is interpolated from the surface of the triangle it falls in. Successive relaxation of the mesh will degrade the original representation of the geometry when the data from Figure 6 are triangulated and smoothed. To illustrate this effect, the average geometry error is plotted for several iterations in Figure 8 for a FASTTABS triangulated mesh. The difference between the reinterpolated line and the smoothed line represents the reduction in error that can be obtained by reinterpolating the relaxed mesh based on the original unrelaxed mesh. One iteration of relaxing the reinterpolated mesh has the same geometry error as the FASTTABS smoothed mesh. The initial jump of absolute average geometry error after one iteration of smoothing benefits the computational properties of the mesh because abrupt features are smoothed, less elements violate the 10 percent slope assumption, and smoothing reduces the number of adjacent elements with 50 percent area change. Experience gained during this research has shown

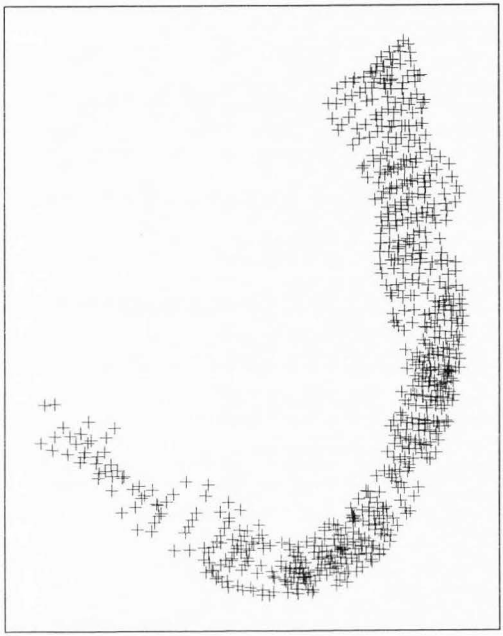

Figure 2. Location of field sampling data based on 749 measurements within the Logan River.

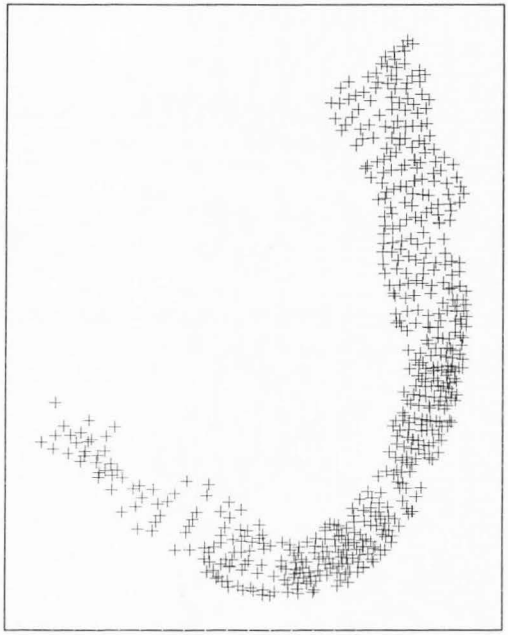

Figure 3. Location of field sampling data based on 575 measurements within the Logan River.

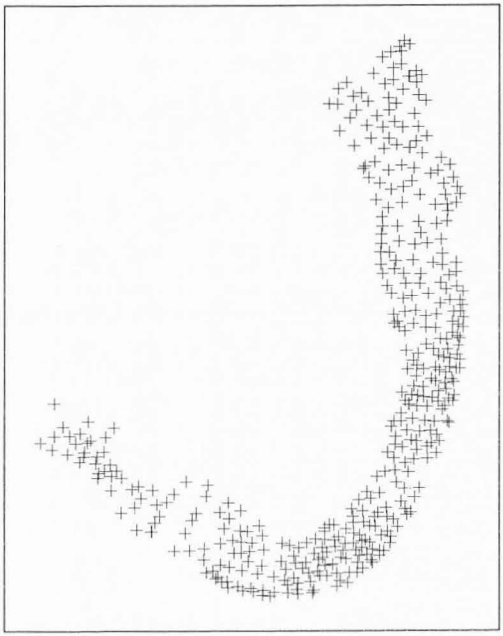

Figure 4. Location of field sampling data based on 415 measurements within the Logan River.

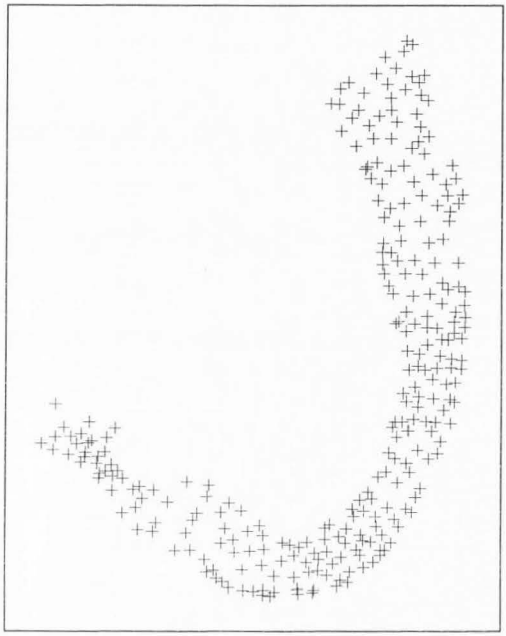

Figure 5. Location of field sampling data based on 283 measurements within the Logan River.

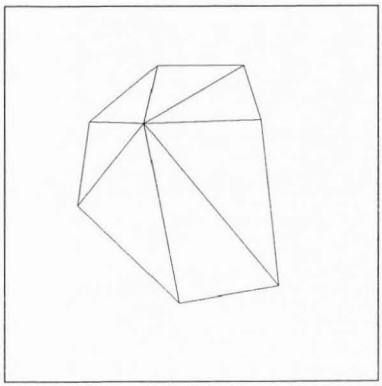

Figure 6. Simple mesh.

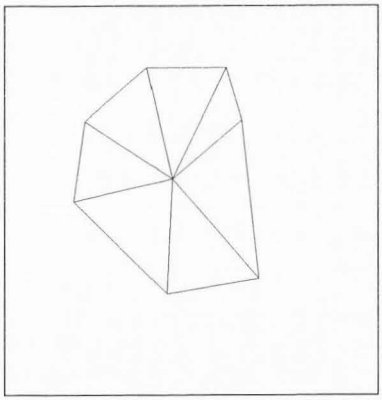

Figure 7. Relaxed simple mesh.

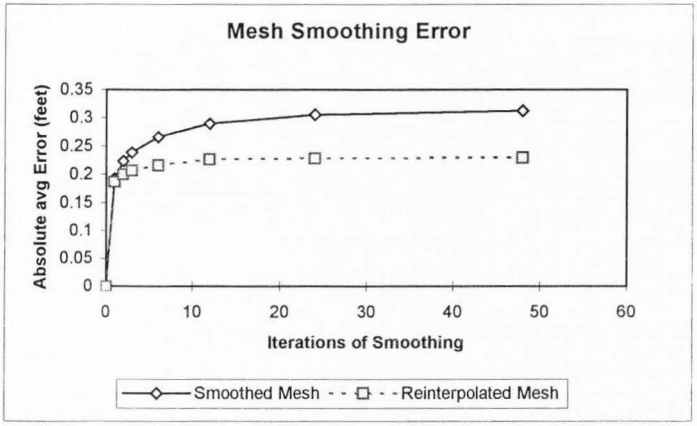

Figure 8. Mesh smoothing error.

that computational instabilities occur in meshes in which an individual element has a slope greater than 10 percent or if adjacent computational elements have differential areas in excess of 50 percent.

CDGMesh

The mesh generation program CDGMesh supports the CDG2D hydraulic program. CDGMesh, developed by Peter Steffler at the University of Alberta Civil Engineering Department, allows smoothing of elements without degrading original geometry as meshes are smoothed to define the nodal elevations in the relaxed computational mesh (Steffler, personal communication, 1997). This software was specifically designed to create meshes

for use with the CDG2D hydrodynamic model. Aside from the preservation of the original geometry points, the CDG2D mesh generation program functions basically the same as the FASTTABS mesh generation program.

To illustrate the differences between FASTTABS and CDG2D mesh generation compared to original field data, Figures 9 through 11 visually show how smoothing affects the three-dimensional space of the river bed. As shown in Figure 1, the original geometry data are preserved when triangulating the raw data without smoothing. The FASTTABS-generated mesh in Figure 10 has the same number of nodes and elements as Figure 9, the difference being nodes have been moved to the centroid of surrounding nodes except at the mesh boundaries. Figure 11 shows the CDGMesh-generated mesh. The number of nodes and elements in Figure 11 is independent from the number of input nodes and elements.

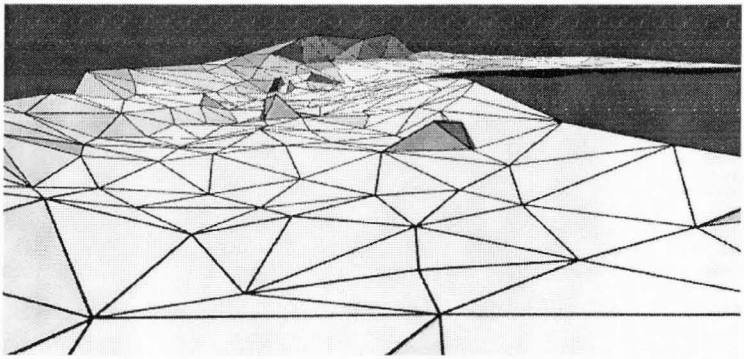

Figure 9. Triangulation of raw field data.

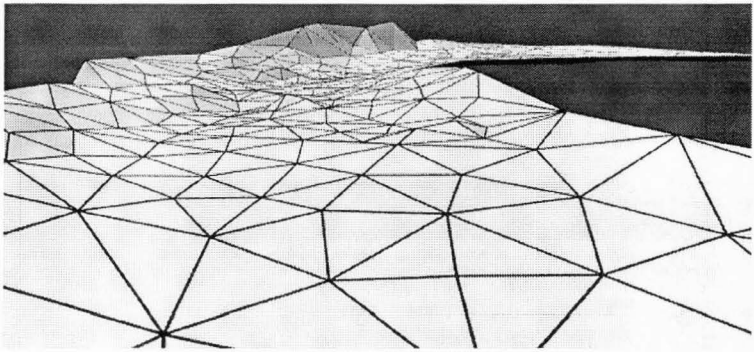

Figure 10. FASTTABS relaxed mesh.

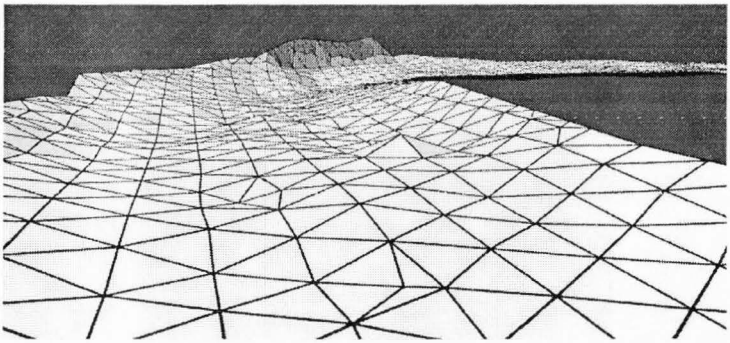

Figure 11. CDGMesh relaxed mesh.

Derivation of Computational Meshes

Four computational meshes were constructed corresponding to the four densities of bed geometry in Figures 2-5. Each of these four computational meshes was constructed to have the same number of nodes and elements resulting in the shape shown in Figure 12. CDGMesh was used to construct these meshes by defining uniform spacing of nodes, combined with a few fixed nodes, and boundary breaklines. The only difference in these four computational meshes is that bed geometry is computed based on the four levels of input geometry. The CDGMesh C++ source code was modified to generate these meshes without the user interface.

For the purposes of model calibration and simulation, all the finite element meshes are extended upstream and downstream of the measured spatial domain in order to place the boundary conditions away from the areas of study as suggested by Ghanem (1995). The extension of the mesh helps in the stability of the solutions, in addition to keeping influence of the boundary condition away from the main portion of the mesh.

Calibration

This class of two-dimensional models was calibrated by adjusting friction and turbulence coefficients. Manning's roughness values and eddy viscosity coefficients are assigned for the RMA2 model at each element. Roughness is assigned and adjusted at each node for calibration of the CDG2D model while the dimensionless eddy viscosity parameter is assigned one value for the whole mesh.

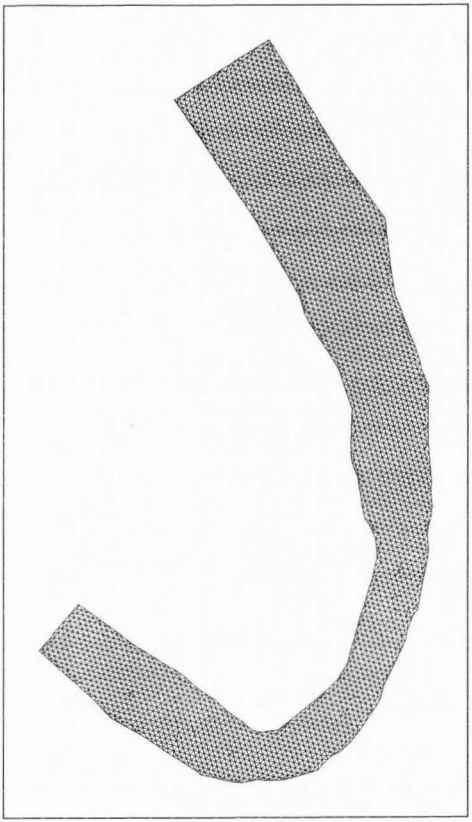

Figure 12. Computational mesh.

Calibration of RMA2

Calibration of the RMA2 model for the Logan River was problematic. A combination of adjusting calibration coefficients and slowly lowering the downstream water surface was required. The actual downstream water surface boundary condition could not be used with RMA2 and obtain a stable calibration. A water surface elevation of approximately 0.5 feet higher than measured was required to obtain solutions that did not diverge during model iterations. Because of the difficulty in calibration of the RMA2 model, an alternative approach was undertaken to the calibration of the Manning's roughness and eddy viscosity coefficients using Monte Carlo simulations to generate random combinations of Manning's roughness and eddy viscosity coefficients in the expected ranges for this type of channel. However, this process did not identify any suitable combinations, which improved the calibration. The best calibration was found by using different roughness values along the edges of the mesh and saving solutions just prior to divergence. The 2.5 percent slope of the Logan River is attributed to the cause of RMA2 model divergence. Figure 13 shows the unstable water surface calculated with RMA2 for the Logan River at the best calibration solution that was obtained. Given this poor model performance, no additional evaluations were undertaken with the RMA2 model.

Calibration of CDG2D

Friction is modeled in CDG2D by applying the steady one-dimensional flow equations to two dimensions. Roughness values (ks) were assigned using a utility called

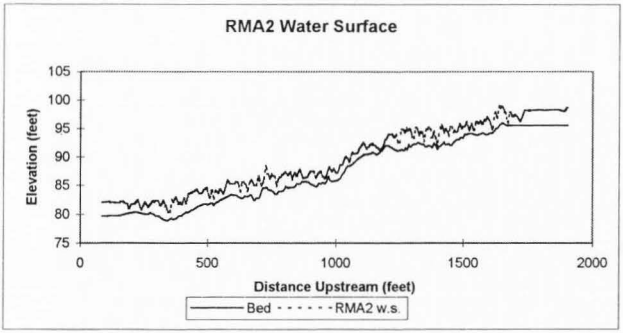

Figure 13. Unstable solution of RMA2 water surface prediction.

"ASSIGNIC.EXE" which assigned initial conditions and roughness values. Input for this utility is a file containing rows of x and y coordinates and the corresponding ks values. In addition, an optional file containing x and y coordinates and the corresponding water surface can be input. Roughness and initial water surfaces are then assigned by node. Each node is assigned the roughness and water surface of the closest corresponding x,y roughness or x,y water surface. Water surface is assigned by calculating the corresponding depth for the water surface by subtracting the elevation from the water surface. Assigning reasonable initial water surfaces decreased computer time significantly during the iteration process. Roughness values were adjusted and the results were viewed one-dimensionally by assigning stations to all data points. Stations were assigned starting downstream and increasing upstream. Profiles computed with a single constant roughness throughout the mesh were attempted, and a value of ks equal to 1.9 proved best with this technique. However, portions of the river being modeled,

particularly runs, were not suited to the same roughness as was needed in riffles or turbulent sections.

An alternative calibration procedure for CDG2G was attempted by variation of the spatial roughness within the study reach based on field observations of the distribution of four substrate classes. The roughness values associated with the spatial distribution of the substrate classes were assigned individual values ranging from 1.9 to 2.5 feet. This procedure was able to replicate the same water surface elevation calibration as obtained from the overall single channel roughness calibration described above.

Calculation of Modeling Errors

Errors for depth, water surface, velocity, and bed elevation were all computed with the same procedure by development of a utility program GE.EXE. This program compares the measured values of depth, velocity, and water surface elevation to the simulated values. It should be noted, the position of measured values will likely not match with computational nodal positions because of smoothing during mesh generation. Depth, velocity, and elevation were interpolated from the computation mesh to match the original x,y position data as measured. Values are interpolated by finding the computational triangle that encompasses the original x,y coordinate and using the equation of a plane based on the three corner nodes.

Both depth and velocity errors were computed by calculating the difference between the field data and the simulated data. By convention, negative errors indicate underprediction by the model. CDG2D allows negative depths (i.e., phreatic surface of

the ground water at the stream margins) and for this application, all nodes with a negative depth and their corresponding velocity were set to zero.

RESULTS AND DISCUSSION

Because the RMA2 model could not be suitably calibrated, only the results based on the CDG2D model will be presented. Note that for the following results and discussion, a given computational mesh remains constant for different simulations.

Geometry Errors

Figure 14 shows the relationship between average absolute geometry error and the number of nodes in the computational mesh based on utilization of all 749 field data measurements. As can be seen in Figure 14, as the number of computational mesh points increases, there is a rapid reduction in the absolute geometry errors. The geometry error becomes somewhat asymptotic at 0.1 feet. Increasing the computational mesh to a larger number of computational elements, however, makes the computational burden too great and exceeds the practical computational capabilities of existing desk-top computer systems. An absolute geometry error of 0.1 feet was considered equivalent to existing practical applied field applications in instream flow assessments utilizing one-dimensional cross-section geomteries. Based on the results in Figure 14, meshes with 3540 computational nodes were utilized in all subsequent simulations.

Figure 15 shows the geometry errors resulting from the four computational meshes generated from a different initial number of field measurements used for the creation of the final computational mesh. These data are also summarized in Table 1.

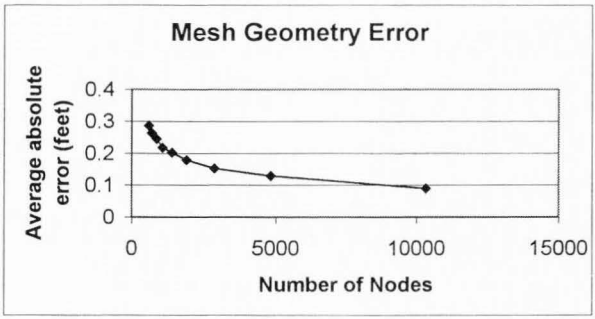

Figure 14. Mesh geometry errors as a function of the number of computational nodes.

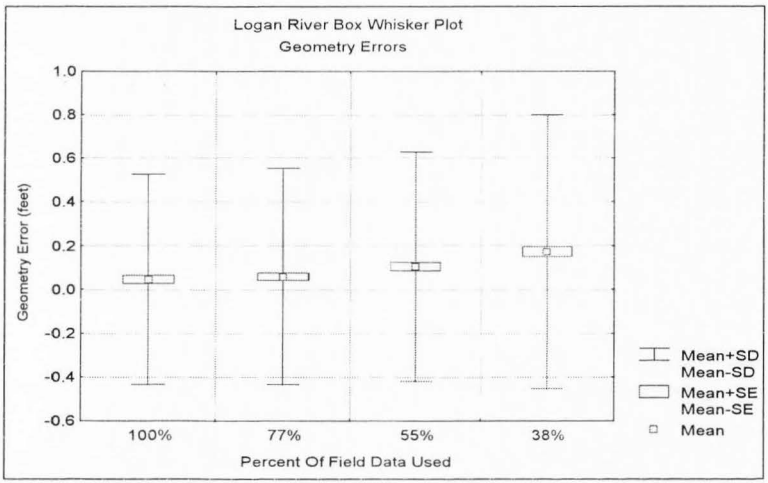

Figure 15. Geometry errors for different levels of field data.

Table 1. Geometry errors (feet) and density statistics

Percent of bed points	100%	77%	55%	38%
Number of points	749	575	415	283
Maximum	2.03	2.03	2.03	4.24
Minimum	-2.27	-2.51	-2.51	-2.87
Standard Deviation (feet)	0.48	0.49	0.52	0.63
Average	0.05	0.06	0.1	0.17
Median	0.04	0.05	0.09	0.13
Points/100 feet^2	2.49	1.91	1.38	0.94
Points/ linear foot	1.22	0.94	0.68	0.46

A comparison of Figure 15 and Table 1 indicates that as the number of field measurement points is increased, an overall reduction in the range of geometry errors is achieved as well as an overall reduction in the magnitude of the average errors. It is also apparent that for these data, little benefit is achieved in terms of error reductions for either the range or averages for 100 versus 77 percent of the data. This lack of incremental benefit is attributed to a small incremental gain in determination of the channel geometry between using all 749 versus 575 field data points. In other words, the channel geometry represented by the 575 data points captures the bed topography adequately while the inclusion of additional data points represents redundant data. The impact of data density in conjunction with mesh generation for channel topographies different than those encountered in this study is at present unknown. It is suspected, however, from experience gained in the analysis of these data that in uniform or homogeneous channel topographies the number of required data points would be substantially less than in highly heterogeneous topographies. The use of a systematic irregular sampling strategy can in part compensate for data collection efforts if a sufficient number of data points are

spatially located to define irregular bed topographies. Figures 16-18 show the range of geometry errors spatially for the 155 cfs data set and the 255 cfs data set. Some of the larger geometry errors occur at locations where several geometry measurements were taken in a relatively small area representing complex channel geometry. Mesh smoothing affects these points considerably since moving nodes, in this densely measured area, to the centroid of surrounding nodes often moves the node a large distance because surrounding nodes are not sampled densely.

Water Surface Elevations at the Calibration Flows

Figures 19-21 show the simulated and measured water surface for this reach of the Logan River calibrated at 155 cfs and 255 cfs. Examination of the calibration data at 155 cfs shows that the model underpredicted the water surface elevations in the steep section located approximately at stationing 1200 in Figure 19. This section of the river is very steep (slope ≥ 0.025) but in the remaining sections with lower slopes, differences between observed and calibrated water surface elevations are in excellent agreement. The only other "problematic" area of the calibration occurs near stationing 1500 where a canal diverts water out of the river. In this area the water surface elevations differ by approximately 1 foot between the left and right banks of the river, and insufficient geometry data were collected to adequately model this effect. The calibration data for 255 cfs shown in Figure 20 and Figure 21 mimic these results with the poorest calibration data occurring in these same two sections of the channel. These results would indicate that although the

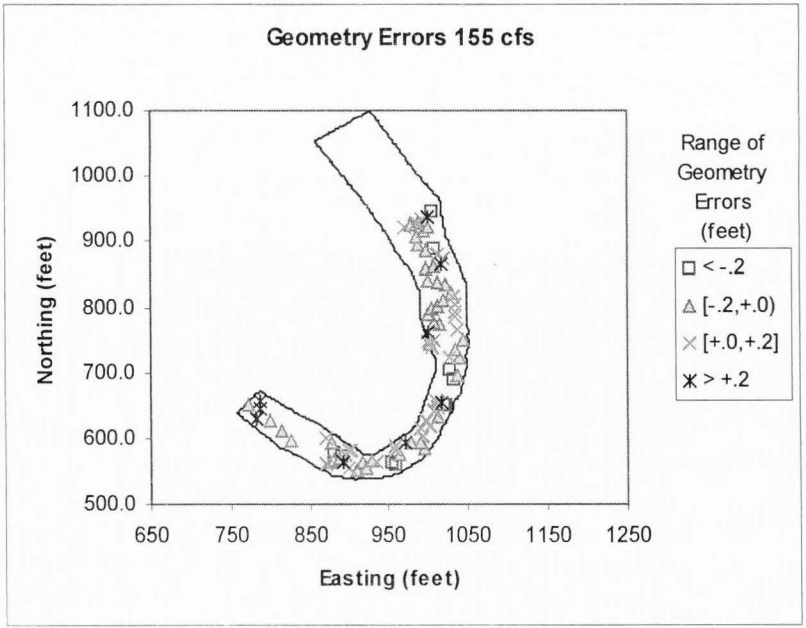

Figure 16. Spatial geometry errors for the 155 cfs data set.

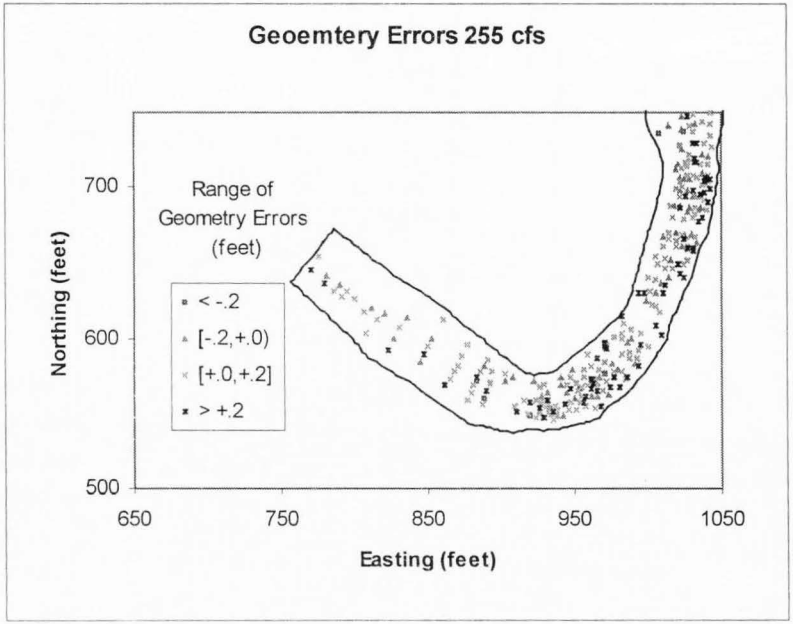

Figure 17. Spatial geometry errors for the 255 cfs data set (downstream).

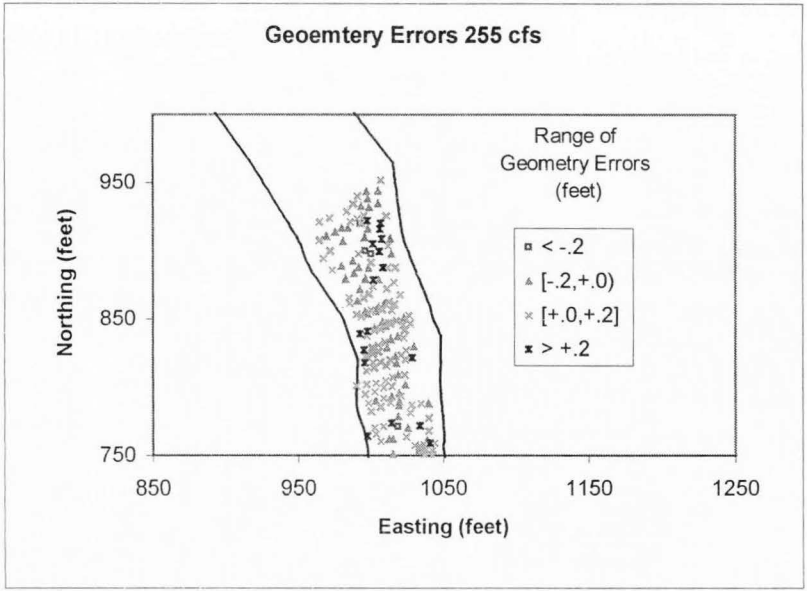

Figure 18. Spatial geometry errors for the 255 cfs data set (upstream).

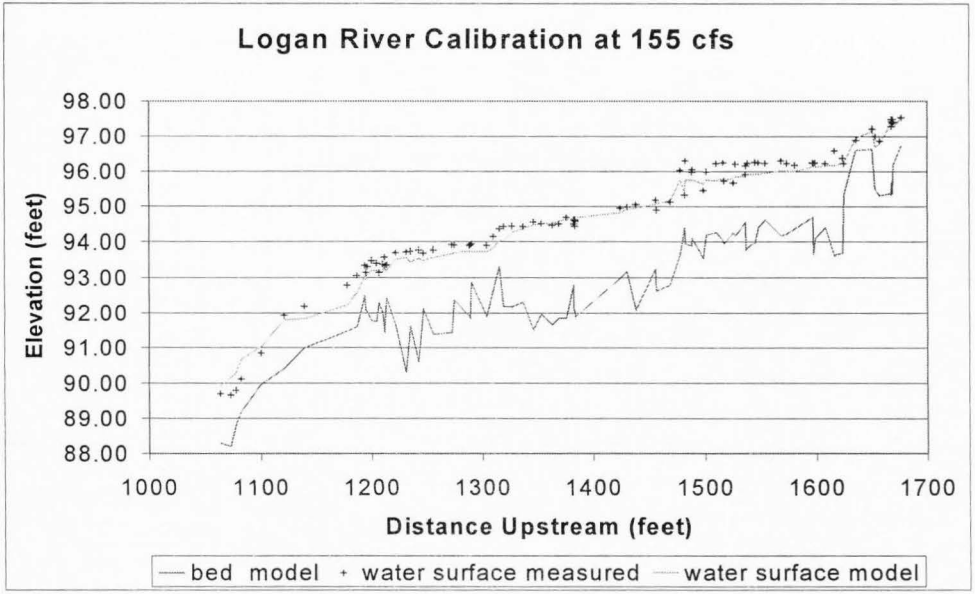

Figure 19. Water surface at the 155 cfs calibration.

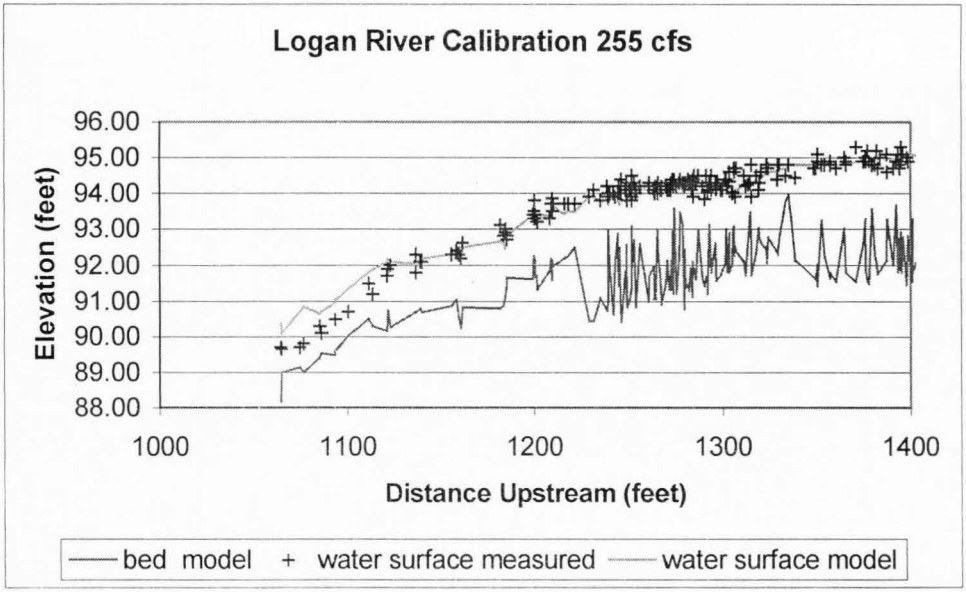

Figure 20. Water surface at the 255 cfs calibration (downstream).

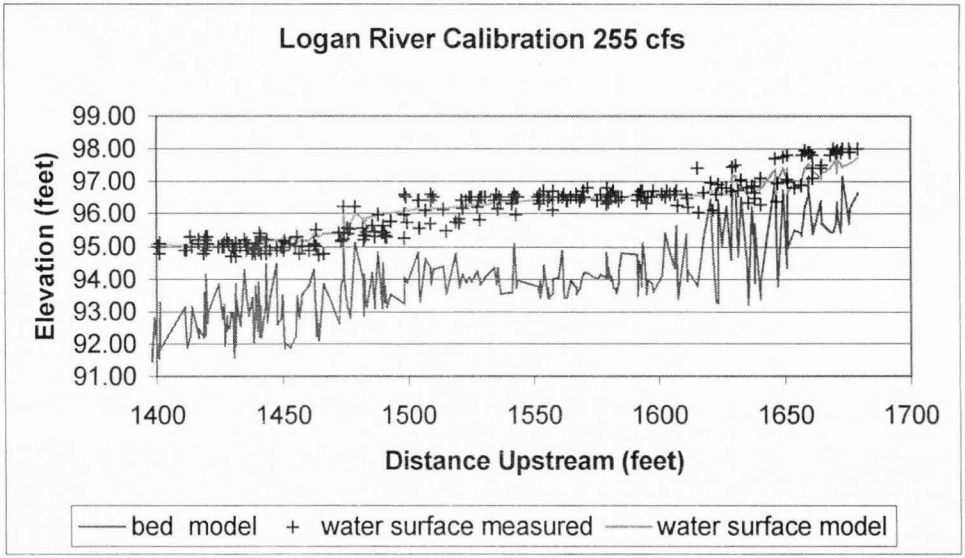

Figure 21. Water surface at the 255 cfs calibration (upstream).

CDG model can handle flow in the steep sections, the complexity of the turbulence and energy loss in this steep section is not at present adequately modeled.

Depth and Velocity Errors at the Calibration Flows

Figures 22 and 23 show depth and velocity errors at the 155 cfs calibration flow for each of the four computational meshes derived from the four different densities of field data measurements. These data have also been summarized in Table 2, which compares calibrated to measured data at 91 available instream measured points. Although as previously demonstrated in Figure 15, which indicated little differences between utilization of 100 versus 77 percent of the field data on geometry errors, the results of depth and velocities do show an incremental reduction in the range and average errors for both depth and velocity. As would be expected from the results of the water surface elevation calibration errors, depths are on average lower than measured and therefore the resulting velocities have positive average errors. This is particularly evident in the examination of the high positive values in the range of the velocity errors. The spatial distribution of depth and velocity errors at calibration flows is presented in Figures 24-29. Better agreement between the calibration water surface elevations would be anticipated to lower both the range and average errors for both the depth and velocity errors. Calibration data at 255 cfs are also summarized in Table 2 for the computational mesh derived from all 749 measured data points and based on a comparison between all available 460 measured depth and velocity data points at this discharge. These data show that at the higher calibration discharge a greater range in the magnitude of the depth and velocity errors

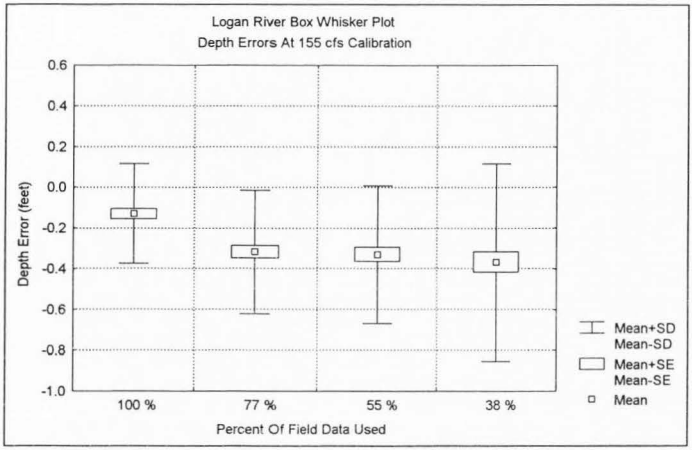

Figure 22. Depth errors at the 155 cfs calibration.

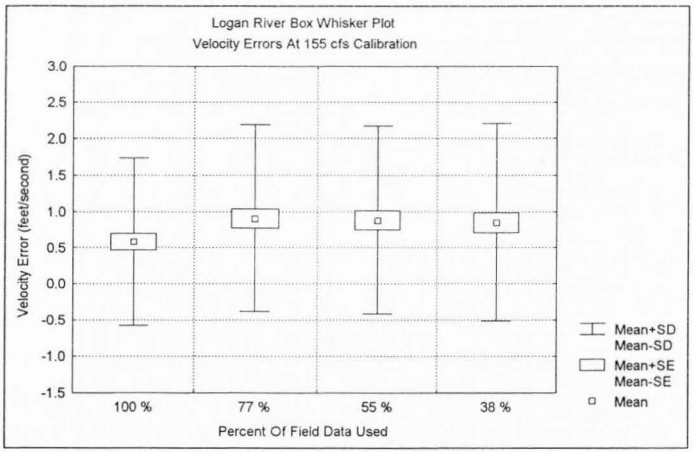

Figure 23. Velocity errors at the 155 cfs calibration.

Table 2. Velocity and depth errors at calibrations of 155 cfs and 255 cfs

Calibration Errors	155 cfs Calibration Velocity					
Percent of bed points	100%	77%	55%	38%		
Number of points	91	91	91	91		
Maximum	3.56	4.07	3.92	4.54		
Minimum	-2.49	-2.41	-2.42	-2.43		
Standard Deviation (feet)	1.15	1.28	1.29	1.36		
Average	0.58	0.90	0.88	0.85		
Median	0.60	1.04	0.99	0.98		
Calibration Errors	155 cfs Calibration Depth				255 cfs Calibration Velocity	Depth
Percent of bed points	100%	77%	55%	38%	100%	100%
Number of points	91	91	91	91	460	460
Maximum	0.50	0.65	0.73	0.90	7.28	1.94
Minimum	-0.94	-1.48	-1.22	-1.62	-3.4	-1.34
Standard Deviation (feet)	0.24	0.30	0.34	0.48	1.53	0.36
Average	-0.13	-0.32	-0.33	-0.37	0.86	-0.04
Median	-0.14	-0.31	-0.35	-0.33	0.79	-0.07

was obtained.

These data suggest that the combination of representation of the bed geometry in the computational mesh and in particular the adequacy of the calibration of the water surface elevations can result in moderate errors in the velocity predictions, especially in steep gradient habitat types. This could have significant impacts on the computation of available or suitable habitat in instream flow applications. Results from the lower gradient sections of the stream, however, suggest that application of this type of modeling can achieve desired model results on par with existing one-dimensional hydraulic simulation programs with the added advantage of more explicit spatial representations.

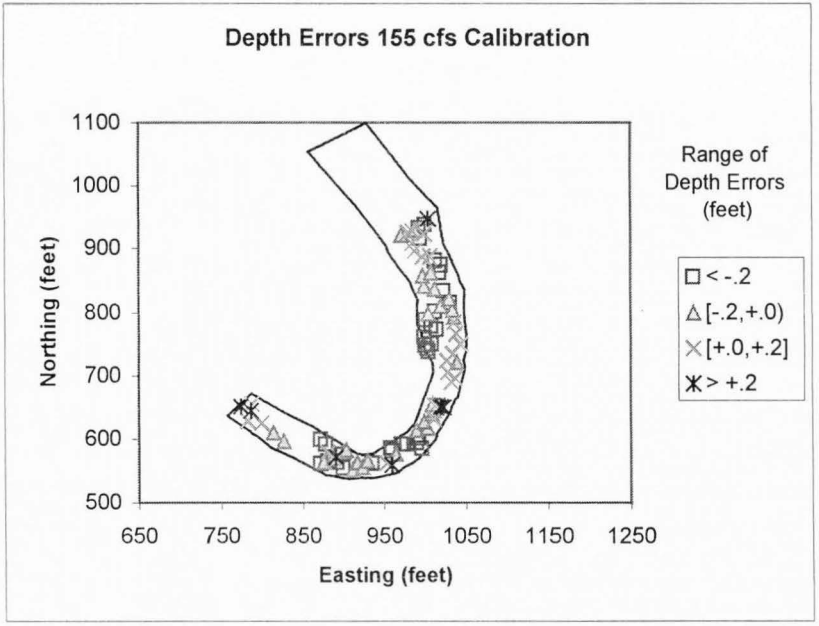

Figure 24. Spatial depth errors at the 155 cfs calibration.

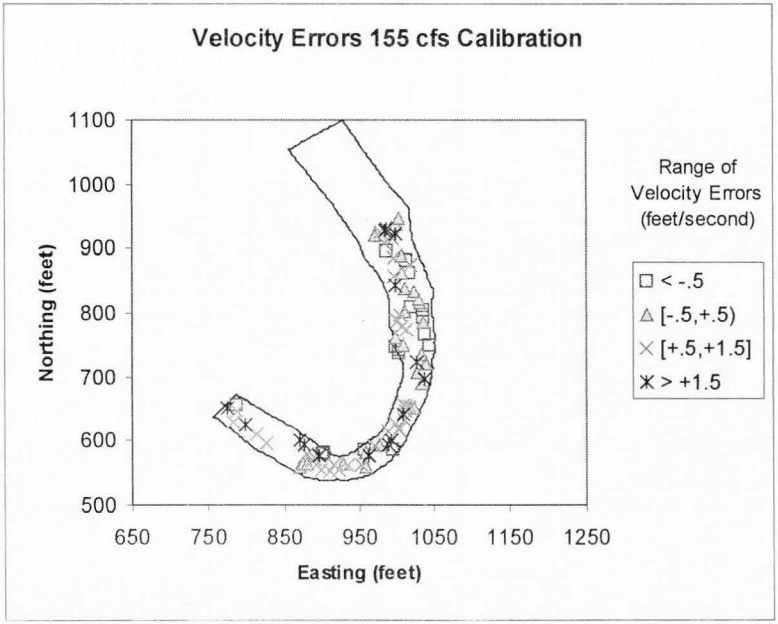

Figure 25. Spatial velocity errors at the 155 cfs calibration.

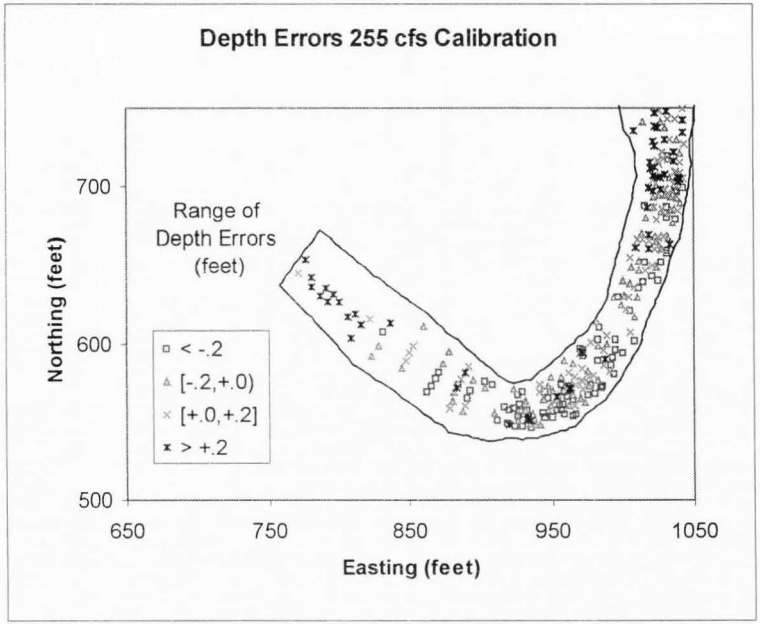

Figure 26. Spatial depth errors at the 255 cfs calibration (downstream).

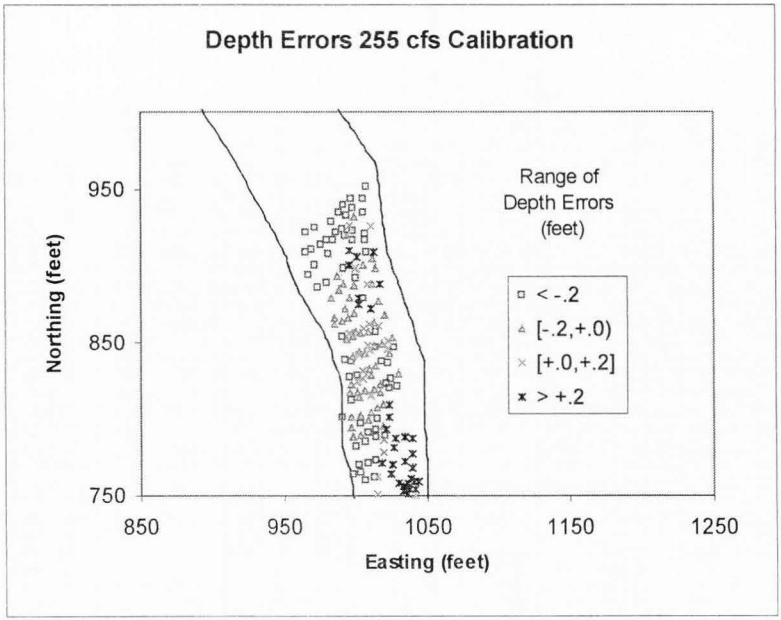

Figure 27. Spatial depth errors at the 255 cfs calibration (upstream).

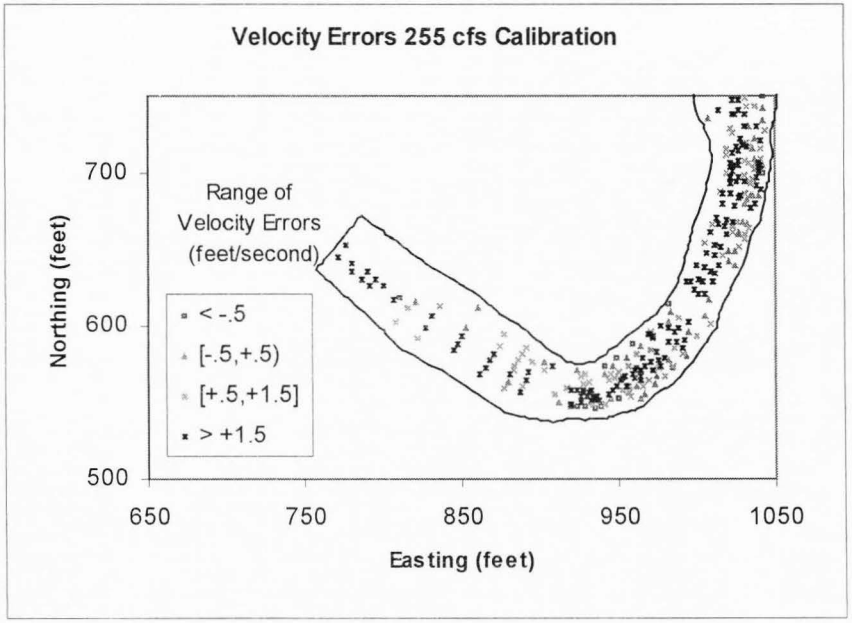

Figure 28. Spatial velocity errors at the 255 cfs calibration (downstream).

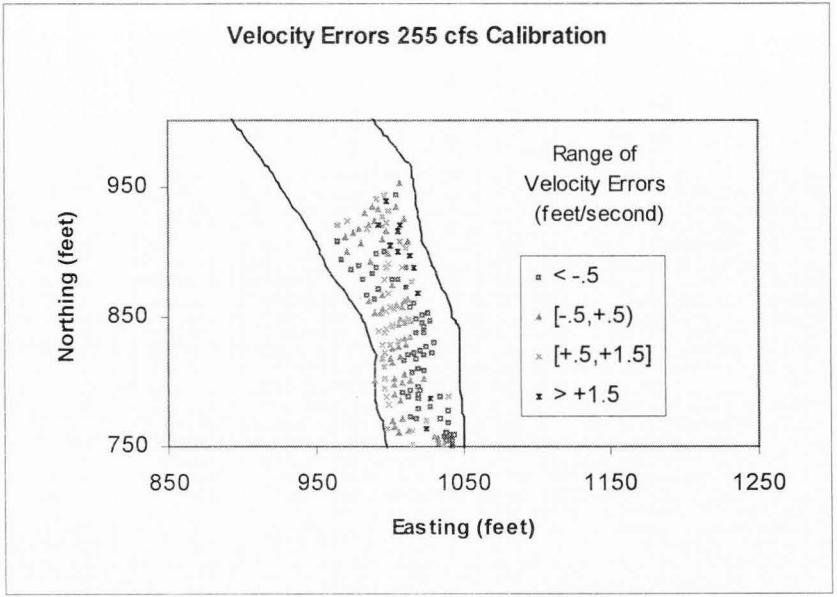

Figure 29. Spatial velocity errors at the 255 cfs calibration (upstream).

Comparison of Measured versus Predicted Errors at Simulated Discharges

Water surface elevations errors

The simulated water surface elevations at 155 and 255 cfs utilizing calibration data at 255 and 155 cfs, respectively, are provided in Figures 30-32. An examination of the data in Figure 30 for the simulated conditions at 155 cfs shows that the water surface elevations are underpredicted over most of the stream channel. This underprediction is attributed to the fact that the roughness values used to calibrate the model at 255 cfs are too low for the simulated conditions at 155 cfs, which results in an underprediction of the water surface elevations. The simulated water surface at 255 cfs is too high based on the calibrated roughness at 155 cfs. This would suggest that the CDG2D model might be improved by incorporating a better variable roughness function with changes in discharge as is currently utilized in the one-dimensional hydraulic simulation routines employed in most instream flow assessments.

Depth and velocity errors

Figures 33-36 show depth and velocity errors for the simulated flow of 255 cfs based on calibration at 155 cfs as well as the simulated flow of 155 cfs based on calibration at 255 cfs. These data are also summarized in Table 3. As would be expected from the results presented above on water surface elevation errors, these results show a rational trend in both depth and velocity errors. The simulated depth and velocity errors at 155 cfs show that the depth errors on average have increased (i.e., more negative) compared to the calibration data and therefore the velocity errors have increased

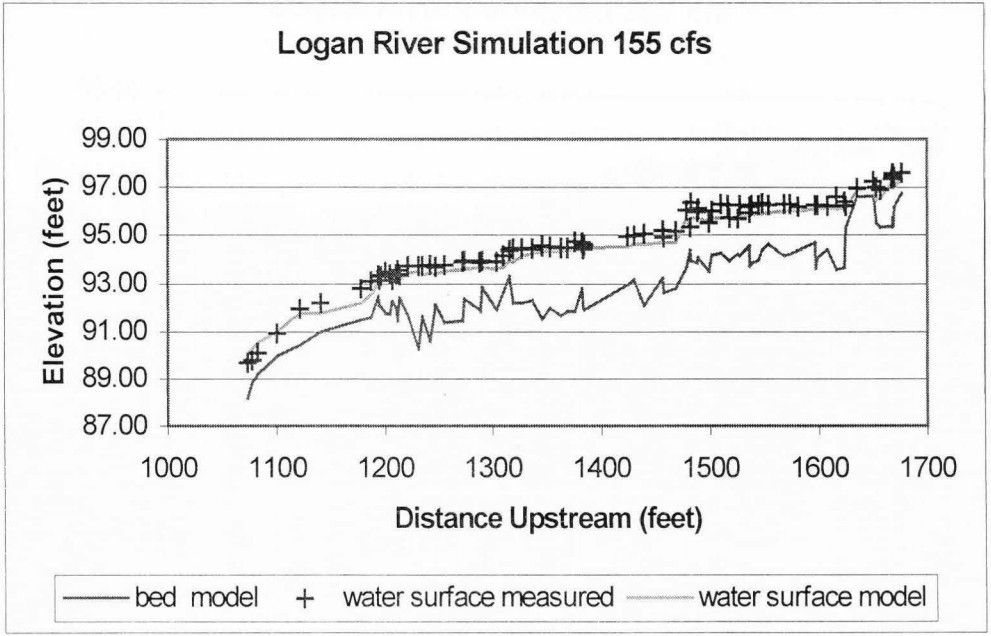

Figure 30. Water surface at the 155 cfs simulation.

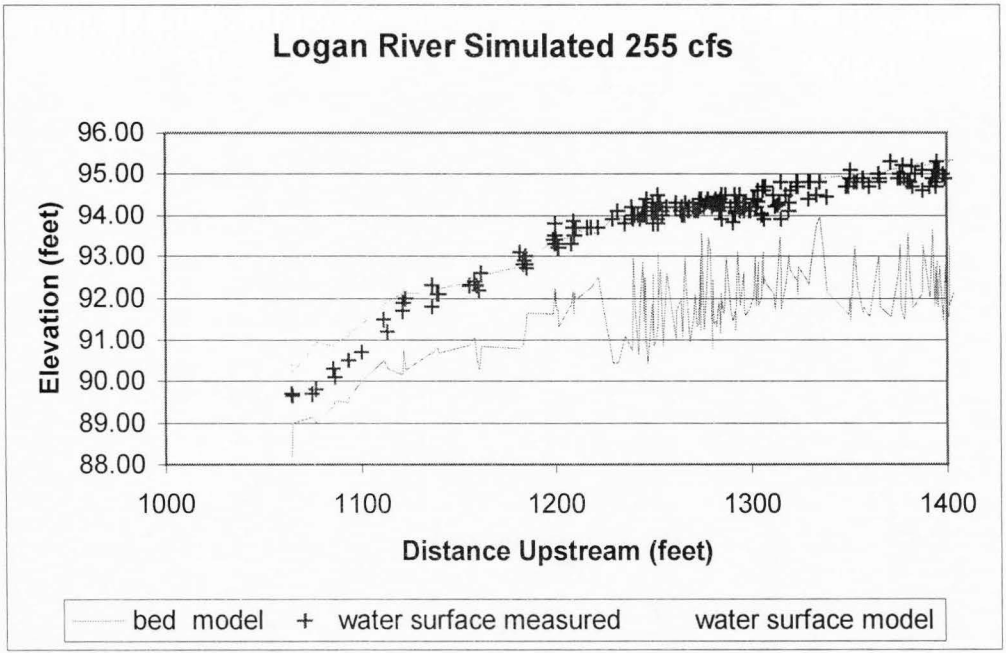

Figure 31. Water surface at the 255 cfs simulation (downstream).

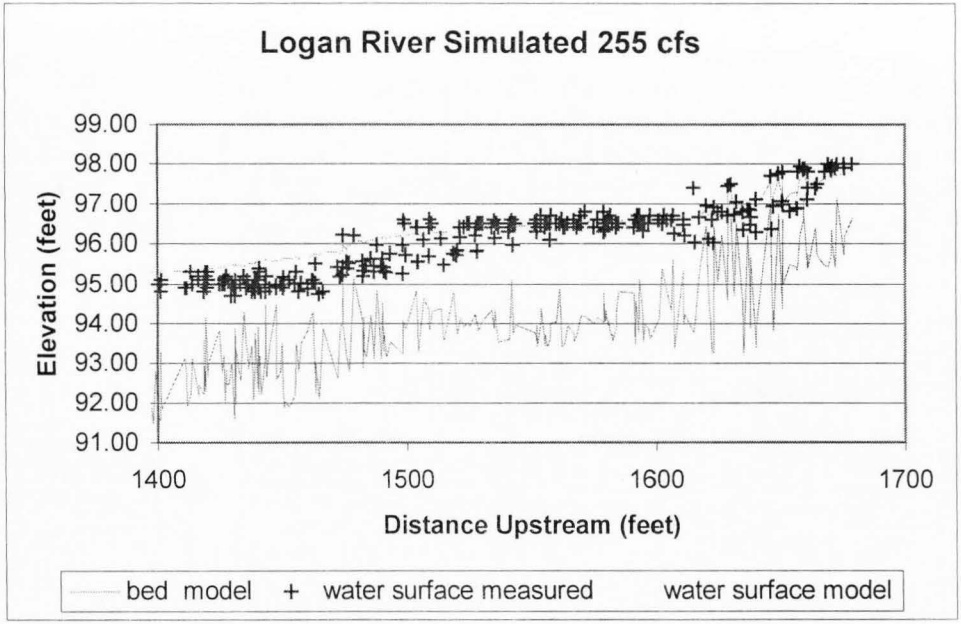

Figure 32. Water surface at the 255 cfs simulation (upstream).

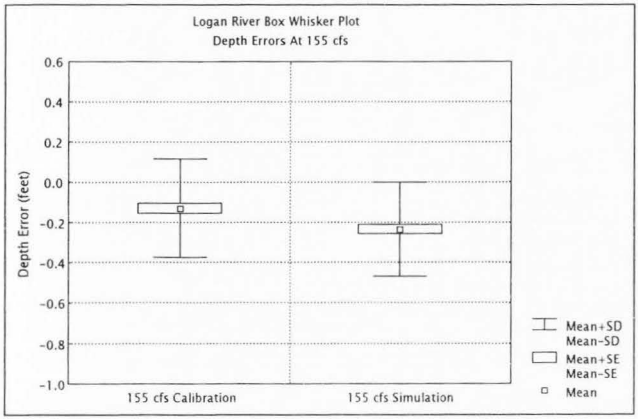

Figure 33. Depth errors at the 155 cfs simulation and calibration.

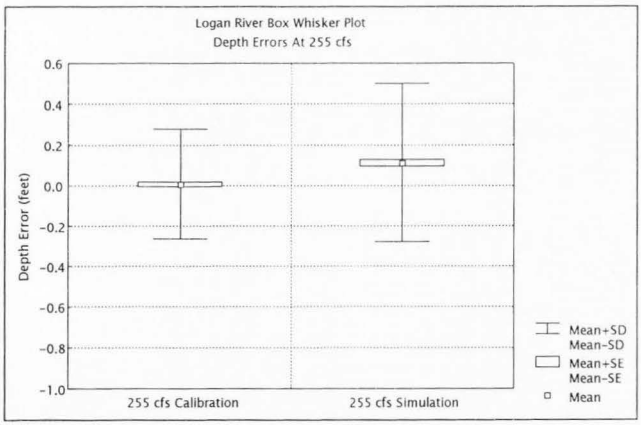

Figure 34. Depth errors at the 255 cfs simulation and calibration.

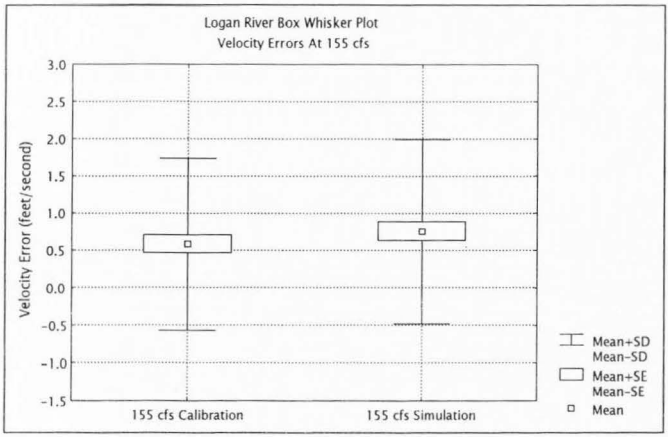

Figure 35. Velocity errors at the 155 cfs simulation and calibration.

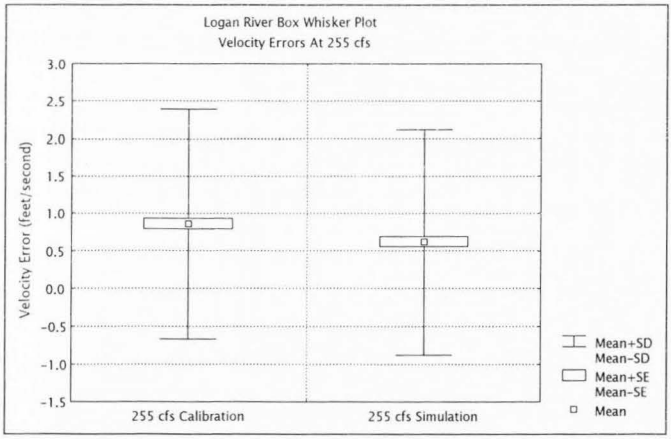

Figure 36. Velocity errors at the 255 cfs simulation and calibration.

Table 3. Velocity and depth errors at simulations of 155 cfs and 255 cfs

Simulation Errors	255 cfs Simulation		155 cfs Simulation	
	Velocity	Depth	Velocity	Depth
Percent of bed points	100%	100%	100%	100%
Number of points	460	460	91	91
Maximum	7.49	1.98	3.92	0.29
Minimum	-3.32	-1.27	-2.41	-1.18
Standard Deviation (feet)	1.50	0.39	1.24	0.23
Average	0.62	0.11	0.76	-0.24
Median	0.59	0.04	0.77	-0.24

in both the magnitude and range with higher overall ranges. In a similar fashion, the results for the 255 cfs simulated flow conditions show that the overall depth errors have increased in both magnitude and range since the water surface elevations are overpredicted. As would be further expected, the increased depth results in some compensation for the velocity predictions and on average velocity errors have been reduced from the calibration errors at 255 although the range in velocity errors are approximately equivalent.

The spatial locations of simulated depth and velocity errors are presented in Figures 37-42. This representation of the data also shows that depth and velocity errors spatially correspond in a logical way.

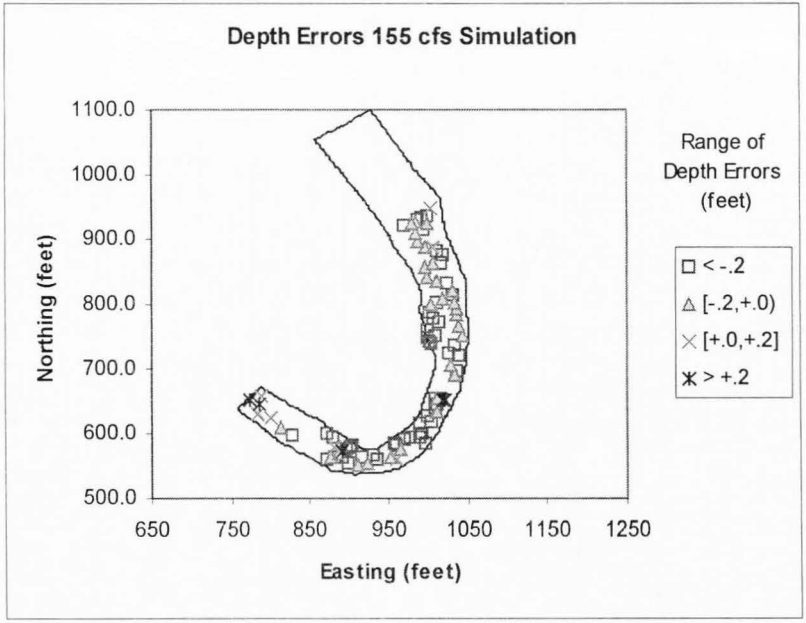

Figure 37. Spatial depth errors at the 155 cfs simulation.

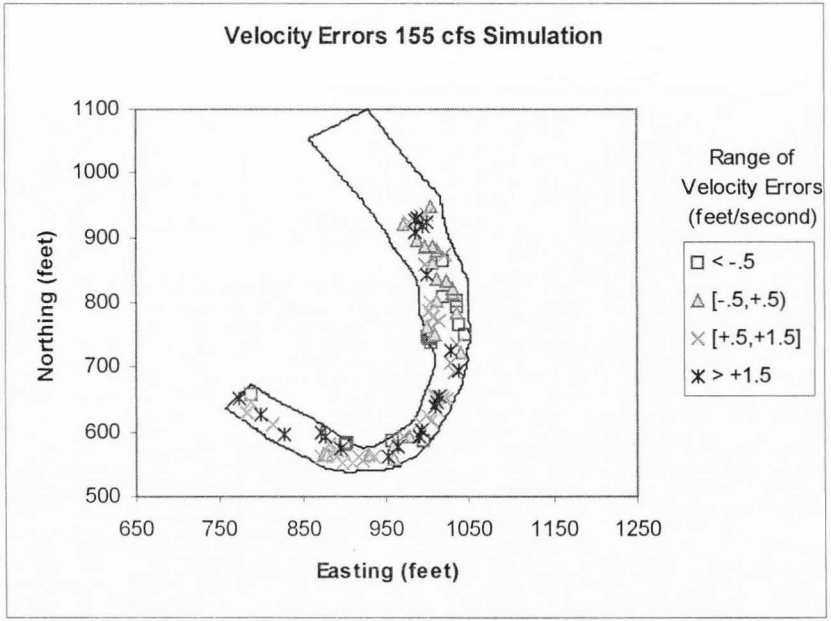

Figure 38. Spatial velocity errors at the 155 cfs simulation.

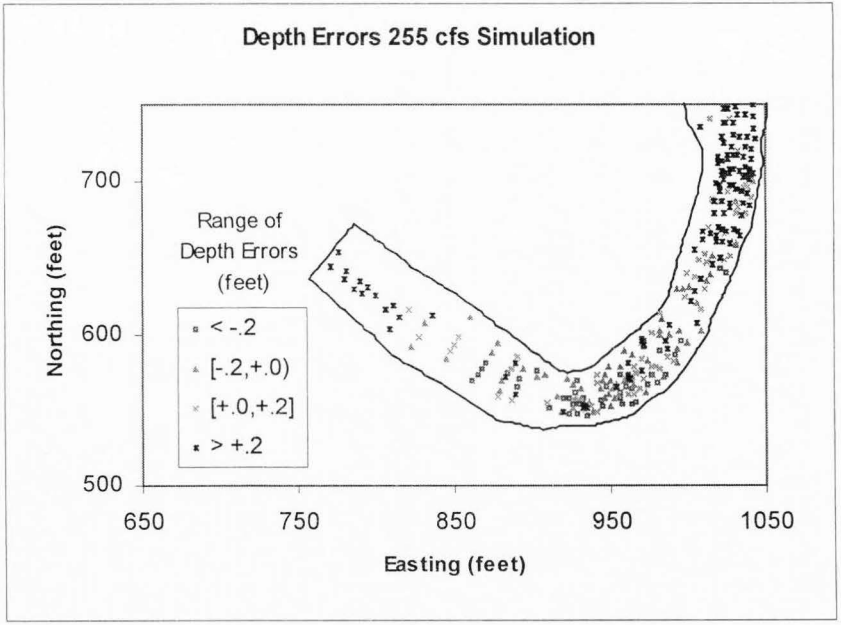

Figure 39. Spatial depth errors at the 255 cfs simulation (downstream).

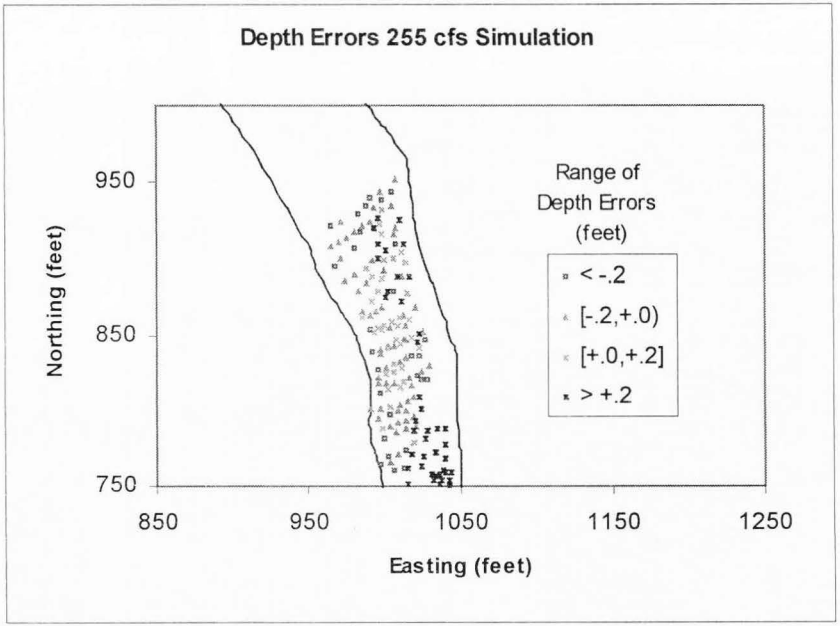

Figure 40. Spatial depth errors at the 255 cfs simulation (upstream).

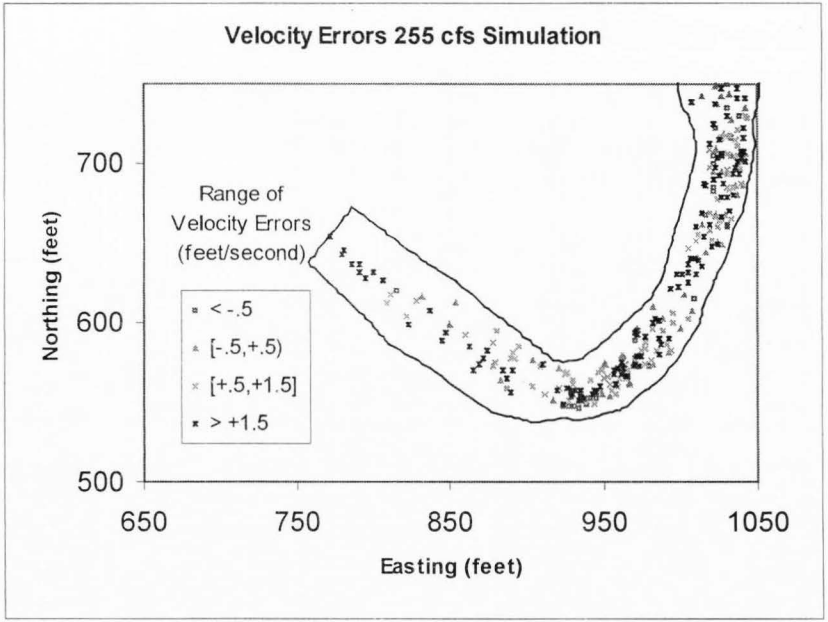

Figure 41. Spatial velocity errors at the 255 cfs simulation (downstream).

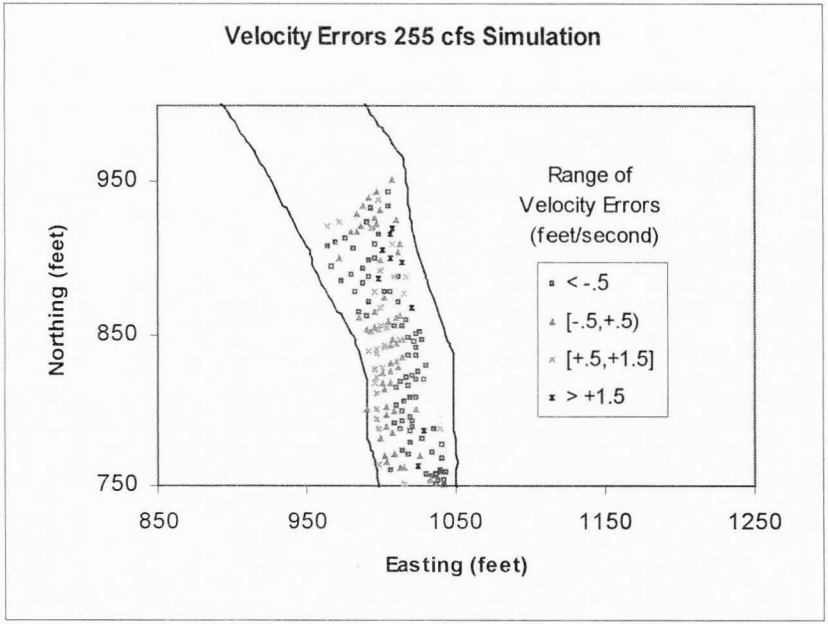

Figure 42. Spatial velocity errors at the 255 cfs simulation (upstream).

Hydraulic Modeling and Calibration

Influence of data collection and roughness assignment on calibration and modeling

Roughness assignment by habitat type such as riffle, run, pool, and turbulent sections worked best with the Logan River. Using polygons to describe actual roughness areas has been shown to be superior using CDG2D (Waddle et al., 1996). Individual roughness assignment by nodes as field data collected did not work well for the Logan River since individual points alone are not collected dense enough to describe areas of substrate or river habitat type. It is also expected that under applied field applications of this type of modeling, substrate mapping across large homogeneous reaches would be most practical and allow for the assignment of roughness using polygons.

By calibrating water surfaces, velocities are not necessarily calibrated by mass balance. The surface area wetted by flow may be more important for velocity calibrations than the actual water surface, particularly with areas of shallow water. Here slight changes in water surface can have a large influence on the surface area. Steffler (personal communication, 1997) has calibrated velocities by matching the wetted perimeter of one-dimensional cross-section data to two-dimensional wetted perimeter data at the same location.

Influence of mesh design on calibration and modeling

"The proper finite element (FE) network is the most fundamental aspect of finite element modeling" (Thomas and McAnally, 1985, p. F-14). However, a proper finite

element network or mesh can be difficult to define. A good mesh represents the physical data and allows optimized computations. These properties of a good mesh can conflict with each other. Unstructured meshes allow using all collected data as the data spatially occur, giving a perfect match in geometry. Unstructured meshes can also result in great difficulties in finite element solutions, depending on the sampling strategies. Meshes built with data collection from the Logan River were reasonable for computations when the meshes were smoothed or generated as a structured mesh, both of which resulted in loss of geometric accuracy. The number of individual elements having slopes greater than 10 percent decreases significantly with smoothing. Depth and velocity errors are expected to have correlation to the quality of the computational mesh.

Computational resources must be considered with mesh design for practical modeling. Increasing nodes over 5000 becomes very prohibitive for computer resources, especially when habitat calculations that require 15-30 simulations to form a range of flows for generation of WUA curves are needed.

Breaklines can be helpful for both calibration and proper modeling. Without using breaklines to control the alignment of elements, flow was constricted, causing backwater effects where none should exist. Even with zero values for roughness calibration, the measured water surface could not be reproduced. Elements that were aligned such that one corner stuck into the wetted portion of the river caused this constriction. By increasing the number of nodes uniformly in the mesh, the constriction was decreased but not eliminated. Breaklines were the best solution for this case. Using breaklines requires additional nodes, but unlike uniformly increasing node density, the additional nodes are

placed in the area of interest only, resulting in fewer nodes but with better results. The use of breaklines preserves geometry features, improves the ability to calibrate, and increases the accuracy of modeling without excess computational effort. Calibration can be extremely dependent on the mesh. Accurate calibration with coarser meshes, however, could not be applied to finer meshes.

Influence of turbulence on calibration and modeling

As described above, accurate calibration was problematic in the steep turbulent section. The lack of headloss resulted in a simulated water surface that was lower than the observed. Calibration of this section results in larger than realistic roughness modeling, which causes problems when simulating other flow rates. The roughness of high gradient rivers (slope greater than one percent) becomes large since boulders form steps, which cause flow to pass through critical depth, such as over rocks (Jarett, 1985; Jeppson, 1993). Using eddy viscosity coefficients does not really model turbulence, especially when the turbulence is near field (Rodi, 1984), which is the case for the Logan River. Additionally, the RMA2 model was designed for far-field problems. The roughness values used in modeling the Logan River with CDG2D were larger than could be physically justified. "Calibration becomes problematic when the physics aren't right" (Steffler, personal communication, 1997).

Implications to Instream Flow Assessments

Calibration of the RMA2 model was problematic in the Logan River given the high gradient and spatially complex changes in channel geometries. Spatial accuracy in the representation of the channel geometries to facilitate computational limitations as well as model instabilities directly affected both the magnitude and spatial distribution of the depth and velocity errors. Study results highlight the importance of careful delineation of complex geometries in terms of meeting a desired data quality objective in the hydraulic simulations and the subsequent representation of the channel geometries given nuances of mesh generation strategies. Although stable solutions of the hydraulics using the CDG2D model were obtained that generated complex flow patterns over the spatial domain, the range and magnitudes of the velocity errors may not be acceptable in light of some applied instream flow assessments. Study results were encouraging in some respects, in that the magnitude of the depth and velocity errors remained fairly constant (i.e., consistent bias) between calibration and simulation discharges. This further suggests that improving model calibrations using a better defined finite element mesh in complex areas of the channel in conjunction with the application of a more robust hydraulic model is likely to reduce the observed errors.

Data collection should be matched to the computational resources available. Data requiring computational meshes over 5000 nodes are likely to be smoothed out in the mesh generation process. Increasing mesh quality with current computational resources requires breaking rivers into smaller reaches for modeling.

RECOMMENDATIONS

Two-dimensional hydraulic modeling provides useful information that cannot be obtained with one-dimensional modeling. However, the benefits of two-dimensional modeling can be expensive. The experience and professional judgment of a hydraulic engineer are needed much more than with traditional one-dimensional modeling. Using two-dimensional modeling assumes attempted modeling of more complicated hydraulics, which are not easy to use with the current software tools. Hydraulic software to visualize and calibrate two-dimensional models is needed. An important part of this software need is user guides explaining the troubles and possible solutions for problems specific to two-dimensional modeling. Limitations of two-dimensional modeling need to be further determined, both in accuracy of depths and velocities modeled under certain types or slopes of rivers. Along with defining the limitations, research is needed to improve turbulence and roughness models to account for the complicated three-dimensional physics of a natural river more completely. Additional research should also include comparison to and quantification of one-dimensional hydraulic modeling capabilities.

Software that allows calibration of two-dimensional models might be designed to incorporate the solution model into the mesh generation interface as an iterative process. Mesh generation could automatically refine the mesh where variables change abruptly, thus capturing important features in depth, velocity, or geometry. Visualization of the effects of mesh generation, as changes are made could also be incorporated into the ideal two-dimensional hydraulic modeling package. Many of these ideal features could be incorporated into powerful geographic information systems (GIS) software packages

currently available. Additionally GIS software packages allow complex data management, which can be used for instream flow assessment calculations such as weighted usable area.

ENGINEERING SIGNIFICANCE

This research has demonstrated both the utility and limitations of the application of two-dimensional hydraulic modeling in terms of its potential application to instream flows. Study results have demonstrated that in a high gradient river with complex geometry, including large roughness elements, the existing models poorly represent water surface elevations, depths, and velocities to a degree that instream flow assessments would be problematic. This research also demonstrated that the existing form of the FASTABS RMA2 hydraulic model is not well suited for higher gradient stream sections where flows approach supercritical conditions.

Although successful calibration of the CDG2D model was achieved in this study, model results were still inadequate in the steeper sections of the stream. Research results also demonstrated that mesh generation can result in the elimination of complex channel geometries in order to obtain a well conditioned computation mesh by smoothing; however, channel complexity cannot be retained unless breaklines or fixed nodes are used. Retention of complex channel geometries results in larger computational meshes, which may then require modeling smaller reaches than desired due to computation limitations of existing desk-top computer systems. With greater computer resources, mesh generation of complex geometry can be improved by increasing the density of the mesh. Collection of data should be at a level consistent with the modeling tools and computational resources.

Research results also indicate that more complete friction and turbulence modeling will be required for steeper and more complex geometry if more accurate representations

of the velocity distributions are necessary, which was found to be a function of water surface elevation modeling. Turbulence modeling research is receiving increased attention by researchers and still remains a complex and computationally intensive research area. Typical roughness models such as Manning's equation are usually used for low gradient channels and this research indicates that alternative approaches to representation and modeling of the roughness will be required in steep gradient systems.

The limitations of mesh generation combined with the limitations of hydraulic modeling need to be more fully understood, and additional research in this area will be necessary.

REFERENCES

Boss International. 1993. Fasttabs users manual. Boss Corporation, Madison, Wisconsin. 192 p.

Bovee, K.D. 1995. A comprehensive overview of the instream flow incremental methodology. National Biological Service, Fort Collins, Colorado. 322 p.

Ghanem, A. 1995. Two-dimensional finite element modeling of flow in aquatic habitats. Unpublished Ph.D. thesis. University of Alberta, Edmondon, Alberta. 105 p.

Ghanem, A., and F. A. Hicks. 1992. A review of the hydraulic models used in instream flow needs assessment methods. Department of Civil Engineering, University of Alberta, Water Resources Engineering Report no. 92-4. 59 p.

Jarett, R.D. 1985. Determination of roughness coefficients for streams in Colorado. U.S. Geological Survey, Water-Resources Investigations Report no. 85-4004. 54 p.

Jeppson, R.W. 1993. Open channel flow utilizing computers. Class notebook. Utah State University, Logan, Utah. 386 p.

Leclerc M., A. Boudreault, J. A. Bechara, and G. Corfa. 1995. Two-dimensional hydrodynamic modeling: A neglected tool in the instream flow incremental methodology. Transactions of the American Fisheries Society 124(5):645-662.

Mathur, D., W.H. Bason, E.J. Purdy, and C.A. Silver. 1985. A critique of the instream flow incremental methodology. Canadian Journal of Fisheries and Aquatic Sciences 42:825-831.

Milhous, R., M. Updike, and D. Schneider. 1989. Physical habitat simulation systems manual--version II. Instream Flow Information Paper no. 26. U.S. Department of the Interior Fish and Wildlife Service Research and Development, Washington, D.C. 383 p.

Orth, D.J., and O.E. Maughan. 1982. Evaluation of the incremental methodology for recommending instream flows for fishes. Transactions of the American Fisheries Society 111:413-445.

Reiser, D.W., T.A. Wesche, and C. Estes. 1989. Status of instream flow legislation and practices in North America. Fisheries (14) 2:22-29.

Rodi,W. 1984. Turbulence models and their application in hydraulics. Second revised edition. Institut Fur Hydromechanik, University of Karlsruhe, Karlsruhe, Federal Republic of Germany. 104 p.

Scott, D., and C.S. Shirvell. 1987. A critique of the instream flow incremental methodology and observation on flow determination in New Zealand, p. 27-43. In J.F. Craig and J.B. Kemper (Eds.). Regulated streams: Advances in ecology. Plenum Press, New York.

Shirvell, C.S. 1986. Pitfalls of physical habitat simulation in the instream flow incremental methodology. Canadian Fisheries and Aquatic Sciences Technical Report no. 1460. 68 p.

Thomas A. W., and W.H. McAnally, Jr. 1985. User's manual for the generalized computer program system open-channel flow and sedimentation TABS-2 main text. Waterways Experiment Station, Corps of Engineers, Vicksburg, Mississippi.

Waddle, T., P. Steffler, A. Ghanem, C. Katopodis, and A. Locke. 1996. Comparision of one and two-dimensional hydrodynamic models for a small habitat stream. Attachment to Procedings EcoHydraulics, June 11-14, Quebec City, Quebec. 12 p.

APPENDIX

155 cfs Field and Model Data												
	<----------Measured---------->					<----------Simulated---------->				<------Calibrated----->		
Station	x-coord	y-coord	elevation	velocity	depth	z	velocity	depth	w.s	velocity	depth	w.s
1063.5	773.6	652.1	88.3	2.8	1.4	88.3	5.4	1.6	89.9	5.1	1.6	89.9
1072.8	787.0	656.3	87.9	4.0	1.8	88.2	1.6	1.9	90.1	1.5	2.0	90.2
1077.5	786.0	645.4	88.6	3.2	1.2	88.8	4.4	1.4	90.2	4.1	1.4	90.3
1082.2	781.9	629.4	88.8	1.2	1.3	89.2	2.3	1.3	90.5	2.3	1.5	90.7
1099.9	798.9	625.6	90.0	2.8	0.9	90.0	5.1	1.0	91.0	5.0	1.1	91.0
1120.9	813.4	610.3	90.5	2.0	1.4	90.4	2.7	1.4	91.8	2.6	1.4	91.8
1139.4	826.3	596.8	91.2	2.1	1.0	91.0	3.8	0.8	91.8	3.6	0.8	91.8
1177.5	871.2	599.7	91.4	0.6	1.4	91.5	3.1	0.7	92.2	3.1	0.8	92.2
1186.3	877.6	592.5	91.7	1.4	1.4	91.6	4.8	0.9	92.5	4.6	1.0	92.6
1193.6	871.4	560.6	92.4	1.9	0.9	92.5	2.5	0.5	93.0	2.3	0.6	93.0
1194.5	880.5	578.9	92.3	2.8	0.8	92.1	3.7	0.8	92.9	3.7	0.8	92.9
1195.7	875.2	564.1	92.1	4.0	1.2	92.0	4.1	1.0	93.1	4.0	1.0	93.1
1199.7	880.0	565.1	91.8	4.0	1.7	91.8	3.8	1.4	93.2	3.7	1.4	93.2
1204.2	886.8	569.4	91.8	3.2	1.6	91.7	4.5	1.4	93.2	4.3	1.5	93.2
1206.5	890.4	571.7	92.5	3.5	0.6	92.3	4.7	0.8	93.1	4.5	0.9	93.2
1210.0	895.9	575.6	92.0	1.9	1.4	92.0	4.1	1.1	93.1	3.8	1.1	93.2
1211.5	892.0	563.1	91.2	3.3	2.4	91.4	4.1	1.9	93.3	3.9	1.9	93.4
1211.9	900.0	580.0	91.8	3.1	1.6	91.8	2.2	1.3	93.1	2.3	1.4	93.2
1213.3	902.6	582.4	92.4	2.0	1.0	92.4	0.6	0.7	93.2	0.8	0.8	93.2
1221.4	898.9	554.1	91.7	1.5	2.1	91.7	2.9	1.8	93.4	2.7	1.8	93.5
1231.1	910.8	551.8	90.3	1.4	3.4	90.3	2.1	3.2	93.5	2.1	3.3	93.6
1234.7	916.5	563.2	91.7	2.1	2.0	91.6	3.6	1.8	93.4	3.5	1.8	93.4
1242.1	922.8	555.7	90.8	2.7	3.0	90.6	4.0	2.9	93.5	3.9	2.9	93.5
1246.6	929.2	566.0	92.2	2.7	1.5	92.1	3.1	1.3	93.4	3.0	1.4	93.5
1255.3	934.8	562.0	91.3	3.0	2.5	91.4	3.8	2.1	93.5	3.7	2.2	93.6
1272.6	953.3	562.5	91.7	2.7	2.2	91.4	4.4	2.2	93.6	4.1	2.2	93.7
1274.0	959.0	559.1	92.9	3.9	1.1	92.4	3.8	1.3	93.6	3.5	1.3	93.7
1288.3	959.1	581.6	91.8	0.9	2.1	91.9	1.1	1.8	93.7	1.4	1.8	93.7
1288.8	963.9	576.6	91.9	0.4	2.0	91.8	3.2	1.9	93.7	3.1	1.9	93.8
1290.0	957.5	586.2	92.7	1.2	1.2	92.9	0.3	0.8	93.7	0.3	0.9	93.7
1303.7	970.4	592.1	91.5	0.3	2.4	91.9	0.8	1.7	93.6	1.7	1.8	93.7
1309.6	977.7	592.5	92.8	4.5	1.4	92.6	4.9	1.1	93.7	4.8	1.2	93.8
1315.3	995.5	585.5	93.4	1.0	1.0	93.3	0.3	0.6	94.0	0.4	0.7	94.0
1319.0	989.7	594.1	92.2	1.1	2.2	92.2	5.0	1.7	93.9	4.7	1.8	94.0
1326.7	992.2	601.4	92.1	1.9	2.3	92.2	3.9	2.0	94.2	3.6	2.1	94.3
1336.7	989.6	614.2	92.2	2.2	2.2	92.3	3.0	2.0	94.3	3.0	2.1	94.4
1346.0	1003.2	617.5	91.5	2.4	3.1	91.5	3.3	2.8	94.4	3.1	3.0	94.5
1353.1	998.9	627.8	91.8	1.6	2.7	92.0	2.9	2.4	94.4	2.8	2.6	94.5
1363.2	1011.4	632.5	91.7	2.4	2.8	91.7	3.8	2.7	94.3	3.6	2.9	94.5
1369.0	1008.3	640.7	91.7	1.6	2.8	91.8	3.6	2.5	94.4	3.2	2.7	94.6
1375.6	1011.3	646.6	91.8	1.7	2.9	91.8	3.3	2.6	94.4	2.9	2.8	94.6
1382.5	1009.2	655.6	92.7	0.9	2.0	92.8	2.1	1.7	94.5	1.9	1.9	94.7
1382.7	1012.6	654.0	92.0	1.3	2.5	92.2	3.1	2.3	94.5	2.8	2.5	94.7
1383.5	1019.3	651.4	92.3	2.9	2.2	92.0	3.6	2.5	94.5	3.2	2.7	94.7
1383.8	1016.4	653.2	91.7	2.2	2.9	92.0	3.6	2.4	94.5	3.2	2.6	94.7

155 cfs Field and Model Data												
	<----------Measured---------->					<----------Simulated---------->				<------Calibrated----->		
Station	x-coord	y-coord	elevation	velocity	depth	z	velocity	depth	w.s	velocity	depth	w.s
1384.1	1022.5	650.3	92.3	2.5	2.3	91.9	3.3	2.6	94.5	3.0	2.8	94.7
1424.2	1032.5	690.4	93.3	4.0	1.7	93.0	4.6	1.5	94.5	3.7	1.9	94.8
1430.7	1037.1	696.3	93.3	0.6	1.7	93.2	3.4	1.4	94.6	2.8	1.7	94.9
1438.8	1027.8	705.9	92.4	3.2	2.7	92.1	4.2	2.5	94.6	3.7	2.9	95.0
1456.1	1039.4	721.7	93.3	3.1	1.9	93.2	3.2	1.5	94.7	2.7	1.8	95.1
1456.9	1026.8	724.3	92.6	0.2	2.3	92.6	3.0	2.1	94.7	2.7	2.5	95.1
1468.4	1034.2	735.0	92.8	4.7	2.3	92.8	5.9	1.9	94.7	4.6	2.3	95.1
1478.0	1003.9	738.8	93.5	0.7	2.5	93.7	0.1	2.1	95.7	0.1	2.1	95.8
1481.5	1043.7	750.3	94.4	2.8	0.9	94.4	1.0	0.9	95.3	1.0	1.0	95.4
1482.4	1002.6	743.0	94.0	0.8	2.4	93.9	0.3	1.8	95.7	0.3	1.8	95.8
1488.2	999.9	748.4	93.9	0.9	2.1	93.9	0.3	1.8	95.7	0.3	1.9	95.8
1488.4	1008.2	750.3	94.0	1.0	2.1	94.1	0.9	1.6	95.7	0.9	1.7	95.8
1498.8	1038.1	766.8	93.4	4.5	2.1	93.5	2.5	2.0	95.6	2.3	2.1	95.6
1501.3	999.2	761.5	93.9	0.0	2.1	94.2	0.3	1.5	95.7	0.3	1.6	95.8
1510.2	1014.1	773.6	94.3	1.5	2.0	94.3	2.1	1.4	95.7	2.1	1.5	95.8
1516.6	1007.3	778.7	94.1	1.1	2.2	94.0	2.3	1.7	95.8	2.2	1.8	95.8
1517.5	1035.3	785.3	93.9	2.1	1.8	94.0	2.0	1.8	95.7	1.9	1.8	95.8
1525.8	1035.4	793.8	94.1	3.4	1.6	94.3	1.6	1.5	95.8	1.6	1.5	95.8
1527.4	1001.3	788.5	94.3	0.8	2.0	94.2	2.1	1.7	95.8	2.1	1.7	95.9
1536.3	1034.3	804.4	94.5	3.2	1.4	94.5	1.5	1.3	95.8	1.5	1.3	95.9
1536.6	1004.2	798.5	93.9	1.0	2.3	93.8	2.2	2.1	95.9	2.1	2.2	95.9
1538.3	1012.1	801.9	93.9	2.0	2.3	93.8	2.3	2.0	95.9	2.3	2.1	95.9
1544.9	1019.4	810.1	94.2	2.8	2.1	94.0	1.9	1.9	95.9	1.9	2.0	95.9
1548.1	1031.0	816.0	94.4	1.2	1.9	94.4	1.3	1.5	95.9	1.3	1.5	95.9
1554.0	1030.1	821.9	94.7	1.2	1.5	94.6	1.2	1.3	95.9	1.2	1.3	95.9
1568.1	1023.1	834.7	94.2	2.2	2.1	94.2	2.4	1.8	96.0	2.4	1.8	96.0
1573.4	1012.0	837.7	94.4	3.1	1.9	94.2	2.9	1.8	96.0	2.8	1.8	96.0
1580.6	999.1	842.2	94.4	0.6	1.8	94.4	2.2	1.6	96.0	2.2	1.6	96.0
1596.6	997.3	858.1	94.7	0.2	1.5	94.7	1.3	1.4	96.1	1.4	1.4	96.1
1597.4	1017.5	863.5	93.4	3.7	2.8	93.6	2.9	2.5	96.1	2.8	2.5	96.1
1598.9	1007.7	862.8	94.2	2.7	2.1	94.1	3.2	2.0	96.1	3.0	2.0	96.1
1603.1	1019.9	875.0	94.2	0.6	2.0	94.4	1.5	1.7	96.1	1.5	1.8	96.2
1616.0	1012.4	881.4	93.5	4.8	3.1	93.6	4.6	2.5	96.1	4.0	2.6	96.2
1623.4	1006.4	887.7	94.0	3.7	2.4	93.7	3.8	2.5	96.1	3.8	2.6	96.2
1624.5	997.8	886.9	95.3	0.2	0.9	95.3	0.6	0.8	96.1	1.2	0.9	96.2
1635.7	987.5	896.0	96.6	1.4	0.3	96.6	1.0	0.3	96.9	0.7	0.3	97.0
1650.2	984.9	908.1	96.7	0.0	0.5	96.6	1.6	0.4	97.0	1.2	0.5	97.2
1653.0	994.6	916.2	95.5	3.3	1.5	95.5	5.9	1.0	96.5	4.6	1.2	96.7
1656.8	999.4	923.0	95.5	3.1	1.4	95.3	6.3	1.2	96.5	5.1	1.5	96.8
1667.5	984.9	927.6	95.3	0.8	2.0	95.4	2.8	1.8	97.2	2.5	2.0	97.4
1667.8	987.5	929.2	95.3	0.6	2.2	95.3	3.0	1.8	97.2	2.7	2.0	97.4
1667.9	978.9	924.9	95.7	1.4	1.7	95.7	2.3	1.6	97.2	2.0	1.8	97.4
1668.1	970.9	921.0	95.6	1.1	1.8	95.7	1.5	1.6	97.3	1.4	1.8	97.5
1668.5	992.8	932.7	95.3	2.6	2.2	95.4	3.4	1.7	97.1	3.0	1.9	97.3
1669.5	1000.0	937.5	95.4	2.5	2.0	96.2	3.3	0.8	97.0	2.4	1.1	97.2
1676.5	1004.1	947.5	97.0	1.0	0.6	96.7	0.8	0.6	97.3	0.8	0.8	97.5

255 cfs Field and Model Data												
	<----------Measured---------->					<----------Simulated---------->				<------Calibrated----->		
Station	x-coord	y-coord	elevation	velocity	depth	z	velocity	depth	w.s	velocity	depth	w.s
1064.6	776.0	654.0	88.1	0.8	1.6	88.2	5.3	2.2	90.4	5.5	2.2	90.4
1065.1	771.3	645.0	88.7	2.0	1.0	89.0	5.2	1.2	90.2	5.5	1.1	90.1
1074.8	780.7	641.9	89.2	0.1	0.5	89.2	5.1	1.6	90.8	5.4	1.6	90.7
1076.6	779.8	636.8	88.8	0.2	1.0	89.0	4.2	1.9	91.0	4.2	1.8	90.9
1085.3	786.4	630.9	89.3	0.4	1.0	89.4	5.4	1.5	90.9	6.1	1.3	90.7
1086.3	790.5	635.8	89.6	2.2	0.5	89.5	6.2	1.4	90.9	7.0	1.2	90.7
1093.3	791.4	627.0	89.4	1.5	1.1	89.5	4.5	1.6	91.1	4.9	1.5	91.0
1093.6	795.4	631.3	89.5	3.4	1.0	89.6	5.7	1.6	91.2	6.1	1.4	91.0
1100.2	800.2	626.7	90.0	3.0	0.7	90.0	6.0	1.4	91.4	6.0	1.3	91.3
1111.3	806.7	617.2	90.5	3.3	1.0	90.5	4.7	1.4	91.9	4.8	1.3	91.8
1113.6	811.5	619.4	90.3	6.4	0.9	90.3	4.6	1.6	91.9	4.7	1.6	91.9
1121.3	815.6	612.3	90.0	3.0	1.7	90.2	3.6	2.0	92.1	3.7	1.9	92.1
1121.6	808.6	603.6	90.7	0.8	1.2	90.8	2.1	1.4	92.2	2.2	1.4	92.2
1123.0	821.4	616.5	90.3	3.3	1.7	90.3	3.6	1.9	92.1	3.7	1.8	92.1
1136.6	831.7	607.5	90.7	2.7	1.6	90.7	4.7	1.4	92.1	4.9	1.3	92.1
1136.6	836.8	613.5	90.7	3.0	1.1	90.7	3.8	1.5	92.2	3.9	1.5	92.1
1139.2	827.8	598.9	90.9	1.4	1.2	90.8	4.9	1.3	92.1	5.2	1.2	92.0
1140.0	823.0	592.0	90.4	2.0	1.7	90.7	2.8	1.5	92.2	2.9	1.5	92.2
1155.8	860.7	612.0	90.7	1.5	1.6	90.9	1.9	1.5	92.4	1.8	1.4	92.3
1158.6	853.5	599.2	91.1	4.2	1.3	91.1	4.0	1.4	92.4	4.1	1.3	92.4
1159.7	850.3	593.8	90.5	2.7	1.8	90.6	4.3	2.0	92.5	4.4	1.9	92.5
1160.8	847.7	589.0	90.0	2.2	2.2	90.2	4.6	2.3	92.5	4.9	2.3	92.5
1161.9	845.2	584.4	90.9	0.1	1.7	90.8	4.4	1.7	92.5	4.4	1.7	92.5
1181.9	862.4	569.4	90.3	0.7	2.8	90.8	2.8	1.9	92.7	2.8	1.9	92.7
1183.5	866.0	573.3	90.7	2.6	2.1	90.9	5.6	1.9	92.7	6.2	1.7	92.6
1184.4	868.8	577.5	91.0	3.2	1.9	91.1	5.2	1.5	92.6	6.5	1.4	92.5
1184.8	871.3	582.1	91.1	1.5	1.9	91.2	4.5	1.5	92.7	5.2	1.3	92.5
1185.3	874.3	587.6	91.4	3.9	1.4	91.4	5.0	1.3	92.8	5.2	1.3	92.7
1185.5	877.9	595.2	91.5	3.7	1.2	91.7	4.9	1.2	92.8	5.1	1.1	92.8
1199.3	881.4	569.4	91.5	3.6	1.9	91.6	5.4	1.8	93.4	5.6	1.8	93.4
1200.0	884.4	574.4	91.5	4.8	1.8	92.3	5.4	1.1	93.4	5.5	1.1	93.4
1200.1	879.8	563.7	91.7	4.3	1.8	91.8	4.6	1.7	93.5	4.7	1.7	93.5
1200.2	883.5	571.9	93.2	5.2	0.6	92.2	5.7	1.2	93.4	5.9	1.2	93.4
1200.5	878.1	559.1	92.0	3.0	1.4	92.1	3.6	1.5	93.6	3.8	1.4	93.6
1200.7	886.7	577.8	91.6	2.9	1.7	91.7	4.0	1.8	93.5	4.0	1.7	93.4
1201.5	889.2	581.5	91.9	2.5	1.3	91.7	3.8	1.7	93.4	4.0	1.7	93.4
1201.8	891.4	585.5	91.2	2.7	2.0	91.3	3.3	2.1	93.4	3.3	2.1	93.4
1208.3	894.8	577.2	91.7	3.7	1.6	91.9	4.4	1.6	93.4	4.7	1.5	93.4
1209.3	892.9	570.5	92.1	3.0	1.6	92.2	5.6	1.3	93.5	5.8	1.3	93.5
1209.7	891.1	565.4	91.1	3.6	2.8	91.6	5.3	2.1	93.7	5.6	2.0	93.6
1209.9	887.4	556.6	92.0	2.5	1.5	92.1	4.4	1.5	93.7	4.6	1.5	93.6
1210.5	889.6	560.2	92.2	4.2	1.5	92.0	5.0	1.7	93.7	5.2	1.7	93.6
1216.5	903.3	576.2	92.1	3.4	1.6	92.2	3.5	1.3	93.5	3.5	1.2	93.4
1218.4	903.6	572.0	92.3	3.6	1.4	92.3	4.2	1.3	93.6	4.3	1.2	93.5
1222.0	908.5	574.2	92.5	0.8	1.2	92.5	2.9	1.1	93.6	2.9	1.0	93.5
1229.4	909.8	555.4	90.4	3.6	3.5	90.4	4.3	3.5	94.0	4.5	3.5	93.9

255 cfs Field and Model Data												
	<----------Measured---------->					<----------Simulated---------->				<------Calibrated----->		
Station	x-coord	y-coord	elevation	velocity	depth	z	velocity	depth	w.s	velocity	depth	w.s
1232.0	911.6	550.7	90.1	2.8	4.0	90.4	2.9	3.6	94.0	2.9	3.5	93.9
1235.6	916.7	559.2	90.9	3.9	2.9	91.1	5.1	2.7	93.8	5.3	2.6	93.7
1239.1	920.0	557.6	90.3	2.8	3.9	90.7	5.0	3.2	93.9	5.2	3.1	93.8
1239.6	919.1	549.3	90.9	0.3	3.1	91.0	3.0	2.9	93.9	3.0	2.9	93.8
1239.7	923.1	571.1	93.0	1.6	0.9	93.0	1.7	0.8	93.8	1.6	0.7	93.7
1240.6	919.9	548.1	93.0	4.7	1.0	91.9	2.3	1.9	93.8	2.3	1.9	93.8
1242.3	923.4	558.2	90.5	2.6	3.5	90.6	4.9	3.3	93.9	5.1	3.2	93.9
1243.3	926.0	567.0	91.9	2.3	2.0	92.0	3.4	1.8	93.8	3.4	1.8	93.8
1244.8	924.0	547.4	92.8	4.0	1.2	92.9	3.4	1.0	93.8	3.3	0.9	93.8
1245.4	927.2	561.8	91.5	3.8	2.7	91.4	4.9	2.4	93.9	5.0	2.4	93.8
1245.8	928.9	569.2	92.4	2.4	1.6	92.5	3.1	1.3	93.8	3.1	1.2	93.7
1246.1	925.9	550.9	91.9	3.6	2.1	91.9	5.0	2.1	93.9	5.2	2.0	93.9
1246.1	926.5	553.8	90.6	2.5	3.4	91.0	5.0	2.9	93.9	5.2	2.8	93.9
1246.6	927.6	557.0	90.7	2.5	3.7	90.5	4.9	3.4	93.9	5.1	3.4	93.9
1246.7	927.8	557.9	90.4	2.3	3.6	90.4	4.9	3.5	93.9	5.0	3.5	93.9
1249.1	931.3	563.9	92.0	3.9	2.1	91.8	5.0	2.0	93.9	5.1	1.9	93.8
1249.6	930.1	554.5	90.9	3.5	3.4	91.0	5.0	2.9	94.0	5.2	2.9	93.9
1249.7	928.9	547.1	92.3	3.6	1.9	92.6	2.3	1.5	94.0	2.3	1.4	94.0
1249.7	930.8	557.5	90.7	3.9	3.1	90.8	5.3	3.1	93.9	5.5	3.0	93.8
1251.1	932.3	558.1	90.8	3.3	3.3	91.0	5.3	2.9	93.9	5.5	2.8	93.8
1252.2	935.1	551.4	91.0	0.5	3.2	91.4	4.0	2.7	94.1	4.1	2.7	94.1
1252.2	932.7	551.6	91.7	0.9	2.2	91.8	4.7	2.3	94.0	4.8	2.2	94.0
1252.2	935.0	546.4	92.9	2.5	1.4	93.1	1.4	1.0	94.1	1.4	1.0	94.1
1252.2	933.6	553.0	92.7	3.3	1.1	91.4	4.8	2.6	94.0	5.0	2.6	94.0
1252.2	934.0	549.4	92.1	3.3	2.0	92.1	3.9	2.0	94.1	4.0	2.0	94.0
1252.2	933.2	554.0	91.5	3.5	3.0	91.3	5.0	2.7	94.0	5.2	2.6	93.9
1252.2	935.0	551.0	92.7	4.5	1.1	91.5	4.0	2.6	94.1	4.1	2.5	94.1
1252.2	933.0	550.7	93.3	4.7	1.0	91.9	4.4	2.1	94.0	4.5	2.1	94.0
1253.4	938.4	548.2	92.8	3.9	1.5	92.7	2.5	1.5	94.2	2.5	1.4	94.1
1254.3	937.9	552.0	90.9	0.6	3.1	91.1	3.5	3.1	94.2	3.6	3.1	94.1
1254.4	936.9	554.7	90.8	2.0	3.3	90.8	4.3	3.3	94.1	4.4	3.2	94.1
1256.6	941.9	548.3	92.6	0.7	1.6	92.6	1.6	1.6	94.2	1.6	1.6	94.2
1261.2	943.6	556.1	90.7	1.3	3.5	91.0	4.2	3.1	94.1	4.4	3.1	94.1
1261.5	945.3	552.7	91.6	4.0	2.7	91.7	3.4	2.5	94.2	3.5	2.4	94.1
1263.8	941.2	568.9	92.1	3.3	2.0	92.0	3.8	2.1	94.0	3.8	2.0	94.0
1264.4	946.5	557.7	90.9	0.5	3.1	91.1	4.4	3.1	94.1	4.6	3.0	94.1
1264.7	944.1	564.2	91.1	3.3	3.1	91.1	4.4	3.1	94.1	4.5	3.0	94.1
1265.8	941.3	574.1	93.0	2.3	1.0	93.0	1.9	1.1	94.1	1.8	1.0	94.0
1266.1	950.4	552.7	92.4	3.6	1.9	92.4	2.8	1.7	94.2	2.9	1.7	94.1
1267.4	944.9	569.4	91.4	2.1	2.7	91.6	3.6	2.5	94.1	3.5	2.5	94.1
1268.0	949.2	560.4	91.1	2.7	3.1	91.1	4.4	3.1	94.2	4.7	3.0	94.1
1268.2	947.2	565.8	90.6	3.3	3.5	90.9	4.1	3.2	94.1	4.2	3.2	94.1
1270.5	953.0	557.7	91.4	3.8	2.8	91.5	4.2	2.7	94.2	4.5	2.6	94.1
1270.9	947.0	573.5	92.1	2.9	2.0	92.1	2.9	2.0	94.1	2.7	1.9	94.1
1272.1	951.9	564.7	91.2	3.5	2.9	91.3	4.8	2.8	94.1	5.1	2.7	94.0
1272.7	950.4	569.9	91.3	2.7	2.8	91.4	3.9	2.8	94.1	4.0	2.7	94.1

255 cfs Field and Model Data												
	<----------Measured---------->					<----------Simulated---------->				<------Calibrated----->		
Station	x-coord	y-coord	elevation	velocity	depth	z	velocity	depth	w.s	velocity	depth	w.s
1273.2	956.1	557.4	91.9	3.0	2.4	92.1	4.1	2.0	94.2	4.4	2.0	94.1
1273.3	954.8	560.9	91.3	2.0	3.0	91.4	4.6	2.8	94.2	4.9	2.7	94.1
1273.5	958.0	554.4	92.9	1.3	1.5	92.9	2.4	1.2	94.2	2.7	1.2	94.1
1274.0	957.2	561.3	91.2	3.4	3.0	91.5	4.5	2.7	94.2	4.8	2.7	94.1
1274.0	953.5	565.9	91.7	2.0	2.5	91.2	4.6	3.0	94.2	4.9	2.9	94.1
1274.3	964.1	553.4	93.4	1.0	1.0	93.6	0.7	0.8	94.3	0.7	0.7	94.3
1275.4	954.3	567.1	91.2	2.2	3.0	91.2	4.4	3.0	94.2	4.6	2.9	94.1
1277.0	961.5	560.8	92.3	4.0	2.0	92.2	4.1	2.1	94.3	4.4	2.0	94.2
1277.7	967.1	555.1	93.2	0.8	1.2	93.5	0.8	0.9	94.3	0.9	0.8	94.3
1279.0	948.9	579.3	93.2	2.2	1.1	93.1	1.8	1.0	94.1	1.5	0.9	94.1
1279.8	960.9	565.9	90.5	2.3	3.7	90.8	4.2	3.5	94.3	4.5	3.4	94.2
1280.1	965.7	560.6	92.5	2.4	1.8	92.4	2.9	1.9	94.3	3.3	1.9	94.3
1280.3	958.8	569.4	91.3	2.1	3.0	91.4	4.3	2.8	94.2	4.5	2.8	94.2
1281.7	956.7	574.1	91.3	2.9	3.1	91.5	3.5	2.7	94.2	3.4	2.7	94.1
1282.1	964.7	564.9	91.0	2.6	3.3	91.3	4.1	3.0	94.3	4.3	3.0	94.3
1283.0	960.7	571.3	92.2	1.4	2.1	91.9	4.7	2.3	94.2	4.9	2.2	94.1
1283.7	962.4	570.3	91.1	4.1	3.0	91.6	4.6	2.6	94.2	4.9	2.5	94.2
1283.9	965.0	567.5	91.0	1.1	3.2	91.1	4.3	3.1	94.3	4.5	3.1	94.2
1284.3	956.0	579.0	92.0	2.3	2.2	92.1	2.7	2.1	94.2	2.4	2.0	94.1
1284.4	962.6	571.2	93.8	5.4	0.6	91.8	4.6	2.5	94.2	4.9	2.4	94.2
1284.5	961.2	573.1	91.1	5.2	2.8	91.8	4.3	2.5	94.2	4.5	2.4	94.1
1284.8	962.2	572.3	94.2	5.4	0.3	91.9	4.6	2.3	94.2	4.8	2.2	94.2
1285.7	969.3	565.1	91.6	2.5	2.7	91.6	3.4	2.7	94.3	3.8	2.7	94.3
1285.9	963.9	572.0	91.7	2.0	2.6	91.7	4.5	2.6	94.2	4.7	2.5	94.2
1287.1	973.3	562.3	93.0	1.6	1.5	93.0	1.7	1.4	94.4	2.0	1.4	94.3
1289.4	966.3	574.5	91.7	2.2	2.5	91.7	4.2	2.6	94.3	4.5	2.6	94.2
1290.5	961.4	582.2	91.3	1.5	2.5	91.4	2.3	2.8	94.2	2.0	2.7	94.2
1291.4	974.7	567.4	91.4	3.0	3.1	91.7	2.8	2.7	94.4	3.2	2.6	94.3
1291.8	965.9	578.9	91.5	2.3	2.5	91.6	3.8	2.7	94.3	3.9	2.6	94.2
1291.9	972.1	571.4	91.1	2.2	3.0	91.2	4.1	3.1	94.3	4.3	3.1	94.3
1292.9	958.8	589.2	93.1	2.5	1.2	93.1	0.2	1.1	94.2	0.1	1.0	94.1
1293.9	970.4	576.7	92.2	3.5	2.3	91.8	4.6	2.4	94.3	4.9	2.4	94.2
1294.0	970.7	576.4	91.9	3.2	2.2	91.8	4.6	2.4	94.3	4.9	2.4	94.2
1296.1	980.2	568.1	92.3	1.0	2.0	92.6	1.4	1.7	94.4	1.7	1.7	94.3
1296.4	964.8	587.3	91.6	1.5	2.5	91.8	2.1	2.4	94.2	1.7	2.3	94.1
1296.6	976.5	573.4	91.4	3.6	2.8	91.6	4.4	2.7	94.3	4.7	2.7	94.3
1297.3	977.1	573.8	91.4	0.6	2.9	91.6	4.5	2.7	94.3	4.8	2.6	94.3
1298.9	970.6	584.2	91.7	3.3	2.4	91.7	4.1	2.5	94.3	4.1	2.4	94.2
1299.7	976.4	578.4	91.8	0.4	2.3	91.8	5.0	2.4	94.3	5.3	2.4	94.2
1301.3	974.9	582.8	92.1	3.5	2.3	92.0	4.9	2.2	94.3	5.3	2.2	94.2
1301.9	984.3	572.3	92.9	3.2	1.5	93.0	1.8	1.3	94.3	2.2	1.3	94.3
1302.4	979.1	579.4	91.9	2.0	2.3	91.8	5.2	2.5	94.3	5.4	2.4	94.2
1303.5	985.4	573.5	92.4	1.5	2.2	92.9	1.7	1.5	94.4	2.0	1.4	94.3
1303.6	982.3	577.4	91.8	5.1	2.5	91.8	4.5	2.5	94.3	4.9	2.5	94.3
1305.0	969.9	594.7	91.8	0.5	2.2	92.0	3.3	2.1	94.2	3.1	2.0	94.1
1305.3	972.0	592.7	91.5	0.3	2.5	92.9	7.8	1.2	94.1	7.6	1.2	94.0

255 cfs Field and Model Data												
	<----------Measured---------->					<----------Simulated---------->				<------Calibrated----->		
Station	x-coord	y-coord	elevation	velocity	depth	z	velocity	depth	w.s	velocity	depth	w.s
1306.0	972.0	593.8	94.4	4.3	0.3	93.1	8.5	1.0	94.1	8.3	0.9	94.0
1306.2	970.8	595.5	94.3	4.4	0.3	92.3	3.9	1.9	94.2	3.7	1.8	94.1
1306.5	970.1	596.8	91.6	2.1	2.3	92.5	2.4	1.7	94.2	2.2	1.6	94.1
1307.3	971.4	596.5	92.4	2.3	2.3	92.4	3.7	1.8	94.1	3.4	1.7	94.1
1311.2	982.3	589.4	92.0	2.5	2.5	92.1	5.2	2.3	94.4	5.5	2.2	94.3
1312.4	986.5	586.1	91.7	4.1	2.5	91.7	5.0	2.7	94.4	5.2	2.6	94.4
1313.5	990.8	582.6	92.7	2.5	1.5	92.7	3.1	1.7	94.4	3.7	1.6	94.3
1314.6	993.4	581.2	93.2	1.4	1.1	93.5	1.4	0.9	94.4	1.7	0.8	94.3
1315.3	991.8	586.5	92.5	1.4	2.3	92.5	4.6	1.9	94.4	5.3	1.8	94.3
1315.3	987.1	590.3	91.7	3.5	2.2	91.7	5.3	2.7	94.4	5.6	2.5	94.3
1317.9	992.8	591.2	92.3	3.1	2.2	92.4	5.2	2.1	94.5	5.7	2.0	94.4
1319.1	977.3	600.7	93.0	3.5	1.1	93.0	5.5	1.3	94.3	5.4	1.2	94.2
1319.3	986.0	596.4	92.9	4.4	1.4	92.7	5.7	1.7	94.4	6.1	1.6	94.3
1320.3	982.3	599.4	92.6	3.5	2.0	92.6	5.3	1.9	94.5	5.4	1.8	94.4
1323.2	982.4	602.7	92.3	4.3	2.4	92.4	4.4	2.2	94.7	4.5	2.2	94.6
1323.3	988.4	599.6	92.6	3.5	2.2	92.5	4.8	2.1	94.7	5.1	2.1	94.6
1323.5	995.3	596.2	91.8	4.5	3.0	92.1	4.2	2.6	94.7	4.5	2.5	94.6
1324.0	999.8	594.4	92.6	2.5	2.1	92.7	3.0	1.9	94.7	3.4	1.9	94.6
1329.1	988.3	606.2	92.3	3.5	2.1	92.3	4.4	2.4	94.7	4.6	2.3	94.6
1329.2	994.5	603.1	92.3	1.5	2.5	92.3	4.8	2.4	94.7	5.1	2.3	94.6
1330.1	983.2	610.1	92.6	3.2	2.2	92.8	3.3	2.0	94.8	3.2	1.9	94.7
1333.5	981.7	614.7	93.5	2.3	1.0	93.8	1.4	1.0	94.8	1.5	0.9	94.7
1334.9	1008.6	602.1	93.7	0.5	1.1	94.0	1.7	0.9	94.9	1.4	0.8	94.8
1338.5	1005.4	607.8	91.9	3.0	2.5	92.2	3.0	2.8	94.9	3.2	2.7	94.8
1348.3	1007.9	617.6	91.5	3.6	3.2	91.7	3.3	3.3	95.0	3.5	3.1	94.8
1349.7	1002.0	622.3	91.6	2.3	3.1	91.6	4.3	3.3	95.0	4.5	3.2	94.8
1350.4	998.7	624.9	92.1	2.3	2.8	92.0	4.0	2.9	95.0	4.2	2.8	94.8
1350.5	1005.6	621.3	91.4	2.4	3.7	91.4	4.1	3.5	95.0	4.3	3.4	94.8
1352.6	993.5	630.1	93.0	0.5	1.8	93.2	2.3	1.8	95.0	2.3	1.6	94.9
1354.2	996.9	630.1	92.0	1.5	2.8	92.3	3.0	2.7	95.0	3.1	2.6	94.9
1357.2	1001.1	631.2	91.5	2.0	3.4	91.6	3.7	3.4	95.0	3.9	3.2	94.9
1357.3	1004.6	629.5	91.8	2.6	3.0	91.8	4.3	3.2	95.0	4.6	3.0	94.8
1360.4	1010.6	629.8	91.3	3.0	3.4	91.6	4.4	3.4	95.0	4.7	3.2	94.8
1364.8	1000.1	640.4	93.0	0.6	2.0	93.0	2.7	2.0	95.0	2.9	1.8	94.8
1365.6	1008.5	636.8	91.9	2.9	3.0	91.8	4.5	3.2	95.0	4.8	3.0	94.8
1365.7	1005.1	638.7	91.8	2.2	3.0	91.9	4.0	3.1	95.0	4.3	2.9	94.8
1365.7	1011.9	635.1	91.4	2.6	3.4	91.8	4.6	3.2	95.0	5.0	3.0	94.8
1371.0	1014.5	639.7	91.6	2.0	3.7	91.6	4.2	3.6	95.1	4.5	3.3	94.9
1375.1	1006.5	648.6	92.5	0.9	2.4	92.6	3.1	2.6	95.1	3.3	2.3	94.9
1376.1	1024.5	640.2	92.8	1.8	2.2	93.3	1.9	2.0	95.3	2.0	1.8	95.1
1376.3	1011.8	647.2	91.7	2.0	3.2	91.8	3.8	3.3	95.2	4.1	3.1	94.9
1377.3	1021.1	643.4	91.2	3.5	4.0	91.6	3.1	3.7	95.3	3.2	3.5	95.0
1378.1	1016.5	646.7	91.4	2.8	3.5	91.5	3.7	3.7	95.2	4.0	3.5	95.0
1379.8	1005.1	654.7	93.5	0.4	1.3	93.6	1.6	1.6	95.2	1.6	1.4	95.0
1381.3	1011.1	653.2	92.1	1.3	2.7	92.3	3.5	2.9	95.2	3.8	2.7	94.9
1382.1	1015.9	651.6	92.1	2.6	3.1	92.1	4.1	3.1	95.2	4.5	2.9	94.9

255 cfs Field and Model Data												
	<----------Measured---------->					<----------Simulated---------->				<------Calibrated----->		
Station	x-coord	y-coord	elevation	velocity	depth	z	velocity	depth	w.s	velocity	depth	w.s
1382.6	1020.4	649.7	91.5	3.8	3.2	91.8	3.8	3.4	95.2	4.2	3.2	95.0
1383.9	1024.0	649.3	91.8	3.8	3.2	91.8	3.5	3.4	95.2	3.7	3.2	95.0
1387.4	1027.2	651.6	92.0	2.2	3.1	92.1	3.1	3.1	95.3	3.3	2.9	95.0
1387.8	1009.7	661.3	93.2	0.7	1.4	93.3	2.4	1.9	95.2	2.6	1.7	95.0
1391.2	1018.8	660.3	92.0	2.5	2.7	92.0	4.0	3.2	95.2	4.5	3.0	95.0
1392.6	1010.2	666.5	93.7	0.8	1.2	93.7	1.8	1.6	95.3	1.8	1.3	95.0
1393.6	1022.6	661.0	91.9	3.5	3.2	91.8	4.0	3.5	95.3	4.4	3.2	95.0
1394.2	1014.3	666.1	92.6	1.2	2.2	92.7	3.0	2.5	95.3	3.3	2.3	95.0
1394.4	1026.8	659.7	91.6	4.2	3.1	91.9	3.5	3.4	95.3	3.8	3.2	95.0
1394.9	1031.2	657.9	92.6	1.3	2.7	92.9	2.5	2.4	95.3	2.7	2.1	95.1
1395.2	1018.6	665.0	91.9	2.4	3.0	92.0	3.7	3.3	95.3	4.0	3.1	95.0
1395.5	1026.7	661.0	91.7	4.4	3.4	91.8	3.5	3.5	95.3	3.9	3.3	95.1
1396.2	1031.3	659.4	92.4	1.4	2.7	92.8	2.6	2.5	95.3	2.7	2.3	95.1
1398.1	1023.8	665.5	91.2	3.1	3.8	91.5	3.8	3.9	95.3	4.2	3.6	95.1
1399.0	1033.5	663.9	92.8	1.1	2.1	92.8	1.9	2.6	95.3	2.0	2.3	95.1
1400.6	1025.1	667.6	91.6	3.7	3.4	91.6	3.8	3.7	95.3	4.3	3.5	95.1
1401.0	1022.6	668.4	91.5	2.8	3.5	91.6	3.9	3.8	95.3	4.3	3.5	95.0
1401.2	1019.1	669.1	92.3	2.3	2.5	92.3	3.9	3.0	95.3	4.3	2.7	95.0
1401.2	1013.5	670.0	93.2	0.3	1.8	93.3	2.6	2.0	95.3	2.7	1.7	95.0
1401.3	1031.9	667.3	92.1	2.8	2.9	92.2	2.9	3.1	95.3	3.1	2.9	95.1
1401.4	1029.4	667.8	91.9	4.0	3.2	91.8	3.4	3.5	95.3	3.7	3.2	95.1
1411.0	1016.7	679.4	93.0	0.7	1.9	93.1	2.8	2.2	95.3	3.0	1.9	95.0
1411.3	1035.2	677.0	92.4	1.3	2.5	92.7	2.8	2.7	95.4	3.0	2.4	95.1
1411.8	1024.1	679.1	91.8	2.6	3.1	91.9	4.2	3.5	95.3	4.7	3.2	95.0
1413.3	1030.9	679.6	92.2	4.1	3.1	92.2	3.9	3.1	95.4	4.5	2.8	95.1
1413.9	1037.2	679.3	92.8	0.7	2.2	93.1	2.4	2.2	95.4	2.4	1.9	95.1
1416.4	1027.1	683.3	92.2	3.5	2.9	92.2	4.4	3.2	95.4	5.1	2.9	95.0
1416.4	1032.2	682.6	92.4	4.4	2.8	92.5	3.8	2.9	95.4	4.5	2.6	95.1
1418.5	1021.8	686.2	92.0	2.0	2.8	92.2	4.1	3.1	95.4	4.6	2.8	95.0
1418.6	1017.3	687.0	93.6	0.9	1.2	93.6	2.5	1.8	95.4	2.5	1.4	95.0
1418.8	1027.9	685.6	92.3	3.7	2.7	92.3	4.5	3.1	95.4	5.2	2.7	95.0
1419.1	1034.6	684.9	92.8	4.5	2.4	92.8	3.7	2.6	95.4	4.4	2.3	95.1
1419.3	1021.6	687.0	92.4	2.4	2.9	92.3	4.1	3.1	95.4	4.6	2.7	95.0
1419.3	1015.8	687.9	94.1	0.8	1.1	94.1	1.5	1.2	95.3	1.7	0.8	95.0
1419.8	1039.9	684.8	93.4	1.4	1.5	93.5	1.9	1.9	95.4	1.7	1.6	95.1
1420.0	1031.4	686.3	92.5	4.6	2.8	92.6	4.4	2.7	95.3	5.3	2.4	95.0
1420.2	1036.2	685.8	93.0	3.9	2.1	93.0	3.5	2.4	95.4	4.2	2.1	95.0
1424.5	1040.7	689.5	93.6	0.5	1.4	93.8	2.0	1.6	95.4	2.0	1.2	95.0
1425.9	1021.4	693.7	92.6	1.6	2.4	92.8	3.4	2.7	95.4	3.8	2.3	95.1
1426.5	1038.1	691.9	93.1	1.8	2.0	93.2	3.4	2.2	95.4	4.1	1.9	95.1
1426.8	1025.8	694.0	91.7	2.5	3.3	91.9	4.4	3.5	95.4	5.0	3.2	95.1
1427.6	1034.5	693.5	92.9	4.1	2.3	92.9	4.3	2.6	95.5	5.1	2.3	95.1
1427.6	1030.5	694.1	92.5	3.7	2.7	92.4	4.6	3.0	95.5	5.5	2.7	95.1
1428.5	1032.0	694.8	92.5	4.4	2.6	92.5	4.4	3.0	95.5	5.2	2.7	95.2
1429.4	1021.4	697.3	93.0	1.1	1.7	93.0	3.0	2.5	95.5	3.1	2.1	95.1
1429.8	1035.6	695.6	92.7	4.2	2.3	93.0	4.2	2.5	95.5	4.9	2.1	95.1

255 cfs Field and Model Data												
	<----------Measured---------->					<----------Simulated---------->				<------Calibrated----->		
Station	x-coord	y-coord	elevation	velocity	depth	z	velocity	depth	w.s	velocity	depth	w.s
1430.6	1026.7	697.7	91.6	2.8	3.3	91.6	4.1	3.9	95.5	4.7	3.6	95.2
1431.0	1018.9	699.3	93.8	0.6	0.9	93.9	1.6	1.6	95.5	1.5	1.3	95.1
1431.1	1039.0	696.5	93.2	1.8	1.9	93.6	3.2	1.9	95.5	3.6	1.6	95.1
1431.2	1030.2	697.9	91.7	3.9	3.2	91.9	4.3	3.6	95.5	5.0	3.2	95.2
1431.5	1037.9	697.0	92.9	1.7	2.0	93.3	3.7	2.1	95.5	4.2	1.8	95.1
1433.1	1023.5	700.8	92.4	1.1	2.6	92.5	3.4	2.9	95.5	3.7	2.6	95.1
1434.6	1042.3	699.5	94.0	3.2	1.2	94.3	1.1	1.2	95.5	1.2	0.8	95.1
1435.5	1021.7	703.5	93.3	1.0	1.6	93.4	3.0	2.0	95.5	3.0	1.7	95.1
1435.7	1039.4	701.1	93.2	0.6	1.9	93.3	3.3	2.2	95.5	3.8	1.8	95.1
1436.3	1036.7	702.1	92.8	5.5	2.2	92.9	4.2	2.7	95.5	5.1	2.3	95.2
1437.8	1039.2	703.2	93.3	0.4	1.5	93.4	3.8	2.1	95.5	4.6	1.7	95.1
1438.0	1024.6	705.6	92.8	0.5	2.1	92.7	3.9	2.7	95.5	4.4	2.4	95.1
1438.4	1027.5	705.5	92.1	3.0	2.8	92.1	4.4	3.4	95.5	5.0	3.1	95.1
1439.0	1037.8	704.6	92.6	5.4	2.2	93.1	4.2	2.4	95.5	5.0	2.0	95.2
1439.0	1021.8	707.0	93.9	0.9	1.0	93.8	2.9	1.7	95.5	3.0	1.3	95.1
1439.0	1040.9	704.2	93.5	3.5	1.6	93.7	2.6	1.9	95.6	2.9	1.5	95.2
1439.1	1040.2	704.4	95.0	3.6	0.1	93.5	3.1	2.0	95.6	3.6	1.7	95.2
1439.9	1033.2	706.2	92.3	5.0	2.8	92.4	4.7	3.1	95.5	5.7	2.8	95.1
1440.3	1042.6	705.2	93.7	1.9	1.2	93.9	1.4	1.7	95.6	1.5	1.4	95.3
1440.4	1040.7	705.6	93.1	0.5	1.9	93.5	2.9	2.1	95.6	3.3	1.8	95.3
1440.5	1026.9	707.7	92.1	2.1	2.8	92.2	4.2	3.3	95.5	4.8	2.9	95.1
1440.6	1039.4	706.0	94.5	5.3	0.9	93.2	3.4	2.4	95.6	4.0	2.0	95.2
1441.0	1039.5	706.4	92.7	2.3	2.6	93.2	3.3	2.4	95.6	3.8	2.1	95.3
1441.4	1030.4	708.1	92.1	4.3	2.7	92.2	4.7	3.3	95.5	5.6	2.9	95.1
1443.1	1040.5	708.4	93.0	1.9	2.0	93.2	2.8	2.4	95.6	3.1	2.1	95.3
1443.2	1019.3	711.6	94.5	0.1	0.3	94.5	1.1	1.1	95.6	0.7	0.7	95.2
1443.6	1037.6	709.3	92.7	4.4	2.5	92.6	3.9	3.0	95.6	4.7	2.6	95.3
1444.8	1022.8	712.7	93.4	0.4	1.5	93.4	2.6	2.1	95.6	2.6	1.8	95.2
1447.4	1019.8	715.8	94.6	0.2	0.4	94.5	1.1	1.1	95.6	0.8	0.7	95.2
1447.5	1026.4	714.9	92.5	1.6	2.4	92.6	3.7	3.0	95.6	4.0	2.6	95.2
1449.3	1025.5	716.8	92.7	0.4	2.3	92.8	3.3	2.8	95.6	3.5	2.4	95.2
1449.9	1041.0	715.1	93.4	2.6	1.6	93.5	3.1	2.1	95.6	3.6	1.7	95.2
1450.1	1036.2	716.1	92.3	5.2	2.6	92.4	4.3	3.3	95.7	5.3	2.9	95.3
1450.5	1032.9	717.0	91.7	4.1	3.5	91.9	4.4	3.8	95.7	5.3	3.4	95.3
1450.7	1032.6	717.2	91.5	3.4	3.5	91.9	4.5	3.8	95.7	5.3	3.4	95.3
1450.7	1029.4	717.7	91.9	2.7	3.1	92.0	4.1	3.6	95.6	4.8	3.2	95.3
1452.8	1032.5	719.3	91.4	4.5	3.7	91.9	4.5	3.8	95.7	5.4	3.4	95.3
1455.0	1028.6	722.1	92.1	0.6	2.9	92.2	4.1	3.4	95.6	4.7	3.0	95.2
1455.5	1041.0	720.8	93.5	2.5	1.8	93.5	3.5	2.2	95.7	4.4	1.8	95.3
1456.6	1036.8	722.5	92.8	6.0	2.0	92.8	4.7	2.8	95.6	5.9	2.4	95.2
1457.6	1023.4	725.5	93.6	0.5	1.4	93.5	2.1	2.1	95.6	1.7	1.7	95.2
1460.3	1022.1	728.4	93.8	0.4	1.1	93.8	1.7	1.8	95.6	1.3	1.4	95.2
1462.2	1044.2	727.1	94.2	2.0	0.9	94.3	2.1	1.5	95.7	2.6	1.1	95.4
1463.1	1033.8	729.5	91.9	6.0	3.1	92.2	4.5	3.5	95.7	5.6	3.1	95.3
1463.1	1038.4	729.5	93.0	0.1	2.5	93.0	4.2	2.8	95.8	5.2	2.4	95.4
1464.3	1030.4	730.1	91.8	3.5	3.0	92.1	4.3	3.6	95.7	5.2	3.2	95.3

255 cfs Field and Model Data												
	<----------Measured---------->					<----------Simulated---------->				<------Calibrated----->		
Station	x-coord	y-coord	elevation	velocity	depth	z	velocity	depth	w.s	velocity	depth	w.s
1466.1	1042.6	734.4	93.7	4.3	1.1	93.9	3.1	2.0	95.8	3.8	1.5	95.4
1471.9	1030.4	737.9	92.6	4.1	2.8	92.6	4.5	3.2	95.8	5.6	2.8	95.4
1472.9	1024.6	737.7	94.5	1.0	0.7	93.9	3.4	1.9	95.8	3.6	1.5	95.4
1474.0	1023.1	738.5	94.1	0.2	1.1	94.0	2.8	1.8	95.8	2.7	1.4	95.4
1474.0	1008.1	735.6	95.8	1.0	0.4	95.3	0.9	1.0	96.3	0.7	0.9	96.2
1474.2	1042.7	742.6	93.9	3.5	1.5	94.0	3.0	2.0	96.0	3.4	1.7	95.7
1475.5	1027.6	741.0	93.0	1.6	2.6	93.1	3.9	2.8	95.9	4.5	2.4	95.5
1475.8	1037.5	743.2	93.0	4.1	2.4	93.1	3.9	2.9	96.0	4.7	2.6	95.7
1476.6	1032.2	743.0	92.8	4.1	2.7	92.8	4.1	3.1	95.9	5.0	2.9	95.7
1478.4	1014.2	741.3	95.3	0.9	0.9	95.1	2.8	0.9	96.1	2.6	0.9	96.0
1481.8	1042.5	750.4	93.9	3.6	1.7	94.1	2.6	2.0	96.1	2.8	1.8	95.9
1482.0	1030.9	748.3	92.7	3.3	2.5	92.9	3.6	3.1	96.0	4.2	2.9	95.8
1482.4	1023.2	747.1	94.2	1.2	1.1	94.2	3.4	1.8	96.0	3.9	1.6	95.7
1482.5	1026.4	747.9	93.0	0.9	2.3	93.3	3.4	2.7	96.0	3.9	2.4	95.8
1483.3	1037.0	750.8	93.1	4.1	2.3	93.1	3.5	2.9	96.1	4.1	2.7	95.9
1485.4	1042.3	754.0	94.1	3.9	1.5	94.2	2.7	1.9	96.1	2.9	1.7	95.9
1486.6	1033.1	753.4	93.1	3.9	2.2	93.1	3.5	3.0	96.1	3.9	2.8	95.9
1486.6	1038.1	754.4	93.2	5.0	2.2	93.4	3.2	2.7	96.1	3.7	2.6	95.9
1487.8	1015.6	751.1	94.9	1.9	1.1	94.8	2.5	1.3	96.2	2.6	1.2	96.1
1489.5	1033.8	756.5	93.0	4.0	2.4	93.1	3.2	3.0	96.1	3.6	2.9	96.0
1489.9	1044.1	758.9	94.4	3.7	1.2	94.5	1.7	1.7	96.2	1.7	1.5	96.0
1490.4	1036.8	758.0	93.2	4.5	2.2	93.3	3.0	2.8	96.1	3.4	2.7	96.0
1490.6	1040.9	759.0	93.5	4.7	1.8	93.8	2.5	2.4	96.2	2.7	2.2	96.0
1491.4	1030.8	757.8	93.1	3.8	2.2	93.1	3.1	3.0	96.1	3.4	2.8	96.0
1493.0	1038.9	761.1	93.6	4.8	2.2	93.5	2.7	2.6	96.2	3.0	2.5	96.0
1498.2	1025.0	763.6	93.1	0.4	2.2	93.2	2.2	3.0	96.2	2.3	2.9	96.1
1498.3	1015.5	761.8	94.1	1.8	1.9	94.1	2.3	2.2	96.2	2.5	2.1	96.1
1498.4	1007.0	760.2	93.8	2.7	2.8	93.9	2.1	2.4	96.3	2.2	2.3	96.2
1499.0	1013.0	762.0	94.0	2.7	2.5	94.0	2.3	2.3	96.2	2.4	2.1	96.1
1499.4	1040.3	767.9	93.8	3.8	1.9	93.9	2.3	2.3	96.2	2.4	2.2	96.1
1503.9	998.2	764.0	94.5	0.3	1.9	94.8	1.0	1.4	96.3	1.0	1.3	96.2
1504.2	1025.7	769.8	94.1	2.6	1.5	94.0	2.9	2.2	96.2	3.1	2.1	96.1
1504.4	1003.9	765.6	93.7	2.1	2.7	93.8	2.2	2.5	96.3	2.3	2.4	96.2
1504.5	1034.1	771.8	93.1	3.8	2.5	93.3	2.7	2.9	96.2	2.9	2.8	96.1
1506.8	1018.8	771.1	94.9	3.7	1.2	94.6	2.8	1.6	96.2	2.9	1.5	96.1
1508.9	1040.4	777.5	94.2	3.2	1.5	94.3	1.8	1.9	96.2	1.9	1.8	96.1
1508.9	1009.0	771.3	93.9	2.6	2.5	93.9	2.7	2.3	96.3	2.8	2.2	96.2
1509.1	1002.6	770.2	93.7	2.0	2.9	93.8	2.3	2.4	96.3	2.4	2.4	96.2
1510.1	1014.5	773.6	94.1	3.5	2.4	94.3	2.7	2.0	96.3	2.8	1.9	96.2
1513.9	1019.3	778.4	94.4	3.7	1.7	94.4	2.7	1.9	96.3	2.8	1.8	96.2
1515.0	1027.4	781.2	93.4	3.8	2.1	93.5	2.6	2.7	96.3	2.8	2.6	96.2
1518.9	1039.8	787.7	94.9	0.9	0.9	94.8	1.5	1.5	96.3	1.5	1.4	96.2
1520.2	1034.9	788.0	93.7	3.3	2.0	93.9	2.2	2.4	96.3	2.3	2.3	96.2
1520.4	1028.5	786.9	93.7	0.5	2.1	93.8	2.5	2.5	96.3	2.7	2.4	96.2
1521.4	1000.4	782.2	93.9	1.9	2.5	94.1	2.3	2.3	96.3	2.4	2.2	96.2
1521.7	1019.9	786.5	94.3	4.3	1.9	94.1	2.8	2.2	96.3	2.9	2.1	96.2

255 cfs Field and Model Data												
	<----------Measured---------->					<---------Simulated--------->				<------Calibrated----->		
Station	x-coord	y-coord	elevation	velocity	depth	z	velocity	depth	w.s	velocity	depth	w.s
1523.2	1007.3	785.4	93.8	2.9	2.6	93.9	2.7	2.5	96.3	2.8	2.4	96.3
1524.5	1020.4	789.4	94.1	4.6	2.4	94.1	2.7	2.3	96.3	2.8	2.2	96.2
1525.2	1013.8	788.8	93.9	3.6	2.6	93.9	2.7	2.4	96.4	2.9	2.3	96.3
1527.7	998.7	788.3	94.1	1.6	2.1	94.2	2.3	2.1	96.4	2.4	2.0	96.3
1528.0	1003.8	789.6	94.1	2.4	2.3	94.1	2.7	2.3	96.4	2.8	2.2	96.3
1528.4	1021.2	793.6	94.0	5.0	1.8	94.0	2.7	2.3	96.3	2.8	2.2	96.3
1528.7	1009.2	791.5	93.8	3.6	2.7	93.8	2.8	2.6	96.4	2.9	2.5	96.3
1529.3	1014.6	793.2	93.9	3.7	2.6	93.9	2.8	2.5	96.4	2.9	2.4	96.3
1530.6	1019.6	795.5	94.2	4.4	2.3	94.1	2.8	2.3	96.4	2.9	2.2	96.3
1534.4	996.8	794.7	94.3	1.1	2.1	94.3	2.0	2.1	96.4	2.1	2.0	96.3
1535.2	1003.4	796.9	93.8	2.2	2.8	93.8	2.5	2.6	96.4	2.6	2.5	96.3
1535.5	1024.2	801.5	94.4	3.2	1.7	94.3	2.8	2.0	96.4	2.8	1.9	96.3
1536.3	1015.0	800.4	93.8	3.3	2.7	93.8	2.7	2.5	96.4	2.8	2.5	96.3
1536.8	1009.3	799.8	93.5	3.1	2.9	93.5	2.6	2.9	96.4	2.8	2.8	96.3
1541.2	1004.0	802.9	93.5	2.1	2.8	93.6	2.5	2.8	96.4	2.6	2.8	96.4
1541.4	1010.6	804.6	93.5	3.2	2.9	93.6	2.6	2.9	96.4	2.7	2.8	96.4
1541.6	997.5	801.8	94.0	1.1	2.5	94.0	1.9	2.4	96.4	2.0	2.3	96.4
1542.4	990.8	801.1	95.1	0.3	1.5	95.1	0.7	1.4	96.5	0.7	1.3	96.4
1542.9	1023.5	809.0	94.0	3.1	2.0	94.1	2.5	2.3	96.4	2.6	2.3	96.4
1542.9	1015.4	807.2	93.7	3.4	2.8	93.7	2.6	2.7	96.4	2.7	2.6	96.4
1543.9	1019.4	809.1	94.0	4.3	2.5	94.0	2.6	2.5	96.4	2.6	2.4	96.4
1551.6	997.4	812.0	93.6	1.1	2.9	93.8	1.9	2.7	96.5	2.0	2.6	96.4
1552.3	1010.9	815.8	93.5	3.5	2.8	93.5	2.6	2.9	96.5	2.7	2.9	96.4
1552.4	1017.9	817.5	94.0	4.2	2.6	94.0	2.7	2.5	96.5	2.7	2.4	96.4
1552.5	1002.8	814.2	93.4	2.2	3.0	93.4	2.4	3.0	96.5	2.5	3.0	96.4
1554.0	1024.2	820.5	94.0	4.2	2.7	94.0	2.6	2.4	96.5	2.7	2.4	96.4
1554.0	1028.9	821.6	94.2	3.2	2.3	94.4	2.2	2.0	96.4	2.2	2.0	96.4
1555.7	1007.2	818.5	93.4	2.9	3.1	93.4	2.5	3.0	96.5	2.6	3.0	96.4
1555.8	1013.5	820.0	93.7	3.6	2.7	93.7	2.6	2.7	96.5	2.7	2.7	96.4
1556.4	1001.7	817.9	93.4	1.9	3.1	93.4	2.3	3.1	96.5	2.4	3.0	96.4
1557.6	996.1	817.9	93.2	0.4	2.9	93.6	1.6	2.9	96.5	1.6	2.8	96.4
1557.7	1017.4	822.8	94.0	4.2	2.5	94.0	2.8	2.5	96.5	2.9	2.4	96.4
1557.8	1021.6	823.9	94.0	5.0	2.7	94.0	2.9	2.5	96.5	2.9	2.4	96.4
1560.0	1025.0	826.9	93.9	3.6	2.6	94.1	2.6	2.4	96.5	2.7	2.4	96.4
1561.7	1030.0	829.7	94.9	3.7	1.6	94.9	1.9	1.6	96.5	1.9	1.5	96.4
1562.2	996.9	822.8	93.4	1.0	3.2	93.4	1.7	3.1	96.5	1.8	3.0	96.4
1563.1	1001.9	824.8	93.4	2.0	3.0	93.4	2.4	3.1	96.5	2.4	3.0	96.4
1563.5	1006.0	826.2	93.5	2.7	2.9	93.5	2.7	3.0	96.5	2.7	2.9	96.4
1564.8	1011.3	828.7	94.0	3.4	2.5	94.0	3.0	2.5	96.5	3.1	2.5	96.4
1567.1	995.8	827.6	93.5	0.4	3.0	93.7	1.6	2.8	96.5	1.6	2.7	96.4
1567.2	1001.4	828.9	93.5	1.6	3.1	93.5	2.4	2.9	96.5	2.5	2.9	96.4
1568.4	1006.0	831.2	93.7	2.4	2.7	93.7	2.9	2.8	96.5	3.0	2.7	96.4
1569.3	1010.3	833.1	94.0	3.5	2.5	94.0	3.2	2.5	96.5	3.3	2.4	96.4
1570.0	1023.3	836.7	94.0	5.4	2.7	94.2	2.9	2.3	96.5	3.0	2.3	96.5
1570.2	1014.2	834.9	94.2	3.9	2.3	94.2	3.4	2.3	96.5	3.6	2.2	96.4
1571.6	1018.7	837.3	94.2	5.1	2.6	94.2	3.5	2.3	96.5	3.6	2.3	96.4

255 cfs Field and Model Data												
	<----------Measured---------->					<----------Simulated---------->				<------Calibrated----->		
Station	x-coord	y-coord	elevation	velocity	depth	z	velocity	depth	w.s	velocity	depth	w.s
1575.3	1023.7	842.3	93.9	4.3	2.5	94.0	2.7	2.5	96.6	2.8	2.5	96.5
1576.8	997.6	837.9	94.1	1.6	2.5	94.2	2.2	2.4	96.5	2.2	2.3	96.4
1579.0	1022.5	845.8	94.0	4.9	2.3	94.0	2.8	2.5	96.6	3.0	2.5	96.5
1579.1	992.7	839.2	94.5	0.2	1.9	94.8	1.0	1.7	96.5	1.0	1.6	96.4
1579.2	1027.4	847.1	94.6	3.9	2.2	94.7	1.6	1.9	96.6	1.5	1.8	96.5
1579.6	1002.7	841.9	94.0	2.3	2.4	94.1	2.9	2.5	96.5	3.0	2.4	96.5
1579.9	1007.1	843.2	94.0	3.3	2.5	94.1	3.3	2.5	96.5	3.4	2.4	96.5
1579.9	997.9	841.2	94.1	1.5	2.3	94.3	2.3	2.2	96.5	2.3	2.1	96.5
1580.8	1010.5	844.9	94.1	3.8	2.5	93.9	3.4	2.6	96.6	3.6	2.6	96.5
1581.0	1002.9	843.4	94.1	1.9	2.5	94.1	2.9	2.4	96.5	3.0	2.4	96.5
1581.8	1014.1	846.8	93.7	3.7	3.0	93.7	3.5	2.8	96.6	3.7	2.8	96.5
1582.8	1013.0	847.5	93.6	2.8	2.9	93.7	3.5	2.9	96.6	3.7	2.8	96.5
1582.9	1018.2	848.8	93.5	5.3	3.0	93.6	3.3	3.0	96.6	3.5	3.0	96.5
1584.1	1008.5	847.9	93.9	3.8	2.6	93.9	3.3	2.7	96.6	3.5	2.6	96.5
1584.1	1023.2	851.2	94.3	4.6	2.1	94.3	2.6	2.3	96.6	2.7	2.3	96.5
1585.2	1026.5	853.0	94.7	4.7	1.8	94.8	1.4	1.8	96.6	1.3	1.7	96.5
1591.3	993.9	852.0	94.6	1.5	1.8	94.8	1.3	1.8	96.6	1.1	1.8	96.5
1591.7	1014.4	857.0	93.3	5.0	3.3	93.5	3.8	3.1	96.6	4.1	3.1	96.6
1592.1	998.5	853.8	94.6	1.2	2.0	94.6	2.1	2.0	96.6	2.0	1.9	96.5
1592.9	1003.7	855.8	94.2	2.3	2.5	94.1	2.8	2.5	96.6	2.9	2.4	96.5
1593.2	1008.6	857.2	93.7	4.2	2.8	93.8	3.5	2.8	96.6	3.7	2.8	96.5
1593.5	990.6	853.5	95.0	0.4	1.7	95.1	0.8	1.5	96.6	0.6	1.4	96.5
1594.2	996.1	855.4	94.7	1.4	1.8	94.7	1.6	1.9	96.6	1.5	1.8	96.5
1594.7	1000.6	857.0	94.3	1.5	2.2	94.4	2.4	2.2	96.6	2.3	2.2	96.5
1595.0	1016.8	860.9	93.4	4.9	2.9	93.5	3.8	3.1	96.6	4.1	3.0	96.5
1595.7	1005.8	859.1	94.0	3.2	2.5	94.0	3.3	2.6	96.6	3.4	2.6	96.5
1597.2	1009.9	861.6	93.9	4.4	2.6	93.9	4.1	2.7	96.6	4.4	2.6	96.5
1597.8	1012.8	862.9	93.6	4.7	3.1	93.6	4.2	3.0	96.6	4.6	2.9	96.5
1601.3	1020.6	868.2	94.0	0.9	2.6	94.1	2.7	2.5	96.6	3.0	2.5	96.6
1602.6	985.8	861.7	95.3	0.2	1.2	95.4	0.3	1.2	96.6	0.1	1.2	96.5
1603.2	990.9	863.5	95.2	2.2	1.5	95.2	0.6	1.4	96.6	0.3	1.4	96.5
1604.5	995.5	865.9	94.8	1.0	1.8	94.8	1.2	1.8	96.6	0.6	1.7	96.5
1606.2	999.4	868.5	94.3	0.8	2.3	94.4	2.1	2.3	96.6	1.6	2.2	96.6
1606.9	985.5	866.0	95.6	2.7	1.1	95.6	0.3	1.0	96.6	0.3	0.9	96.5
1607.4	1011.4	872.4	93.2	5.4	3.0	93.4	4.4	3.3	96.7	4.8	3.2	96.6
1610.9	992.6	871.8	95.4	1.3	1.2	95.4	0.4	1.3	96.6	0.3	1.2	96.5
1611.2	1016.1	877.3	93.8	3.4	2.7	93.9	4.3	2.7	96.6	4.9	2.6	96.6
1611.5	1002.1	874.5	94.2	2.8	2.0	94.3	3.0	2.4	96.6	2.6	2.3	96.6
1615.1	1006.0	879.1	93.8	4.8	3.6	93.8	4.2	2.9	96.6	4.3	2.8	96.6
1615.7	1002.3	878.9	93.7	3.6	2.3	94.0	3.0	2.6	96.7	2.5	2.5	96.6
1617.5	996.5	879.4	95.3	0.2	1.4	95.2	0.9	1.4	96.6	0.8	1.3	96.5
1620.4	982.9	879.3	96.5	3.2	0.5	96.4	1.0	0.4	96.9	1.5	0.3	96.8
1621.4	1017.5	888.1	94.6	1.8	1.5	94.7	3.2	2.0	96.7	4.1	1.9	96.6
1622.6	1011.7	888.0	93.1	6.5	3.5	93.3	5.1	3.5	96.7	5.6	3.4	96.6
1623.3	1009.0	888.2	92.8	4.2	3.2	93.3	5.0	3.5	96.7	5.3	3.4	96.6
1623.5	988.7	883.8	96.5	1.9	0.4	96.4	0.9	0.4	96.8	1.3	0.3	96.7

255 cfs Field and Model Data												
	<----------Measured---------->					<----------Simulated---------->				<------Calibrated----->		
Station	x-coord	y-coord	elevation	velocity	depth	z	velocity	depth	w.s	velocity	depth	w.s
1624.9	999.0	887.5	95.2	0.3	1.6	95.1	2.1	1.6	96.7	1.1	1.5	96.6
1626.7	991.9	887.8	96.4	2.3	0.4	96.2	0.9	0.5	96.7	1.5	0.4	96.6
1628.7	1000.5	891.8	94.5	0.9	2.2	94.6	2.3	2.1	96.7	1.5	2.0	96.6
1629.0	973.8	886.1	96.7	3.0	0.8	96.8	0.8	0.6	97.3	0.9	0.4	97.2
1630.4	980.1	888.9	96.7	2.4	0.8	96.7	1.1	0.6	97.3	1.7	0.5	97.2
1631.5	1014.6	897.8	94.7	2.7	2.0	94.7	4.8	2.1	96.8	5.7	2.0	96.7
1632.4	988.1	892.8	96.5	2.2	0.6	96.5	1.4	0.6	97.1	2.2	0.5	97.0
1634.9	1000.4	898.1	94.8	2.0	2.0	94.6	2.3	2.2	96.8	2.1	2.0	96.6
1635.3	1006.1	899.8	92.8	1.3	3.5	93.2	4.7	3.6	96.8	5.1	3.5	96.7
1636.8	991.8	898.1	96.2	4.3	0.7	96.2	1.5	0.6	96.8	2.2	0.4	96.6
1637.9	1013.5	908.6	94.9	3.8	1.6	94.8	3.7	2.2	97.0	3.9	2.1	96.9
1637.9	1012.2	904.1	93.7	3.8	3.1	93.9	4.2	3.1	97.0	4.5	3.0	96.9
1638.0	996.6	900.4	96.0	3.0	0.7	95.7	1.5	1.1	96.7	1.8	0.9	96.6
1640.2	1007.8	908.6	93.0	3.6	4.1	93.4	4.6	3.7	97.0	4.9	3.5	96.9
1640.3	1001.8	905.6	93.7	0.6	2.6	93.9	3.7	3.0	96.9	3.9	2.8	96.7
1646.2	967.5	894.6	96.9	0.9	0.8	97.0	0.4	0.5	97.5	0.4	0.3	97.4
1646.5	996.2	909.7	95.4	4.9	1.0	95.3	4.1	1.6	96.9	5.4	1.3	96.6
1647.1	1006.8	915.8	93.4	2.4	3.5	93.8	3.9	3.4	97.2	4.3	3.2	97.0
1649.2	972.1	900.4	96.7	1.3	1.1	96.7	1.3	0.9	97.6	1.7	0.7	97.4
1650.7	1007.3	920.2	94.1	1.4	3.0	94.4	3.5	2.9	97.2	3.9	2.7	97.0
1650.9	981.0	906.9	96.6	3.1	1.2	96.6	1.9	1.0	97.6	2.6	0.8	97.4
1651.0	998.5	916.0	95.1	7.0	1.9	95.0	5.5	2.0	97.0	6.8	1.7	96.6
1653.7	1011.0	925.4	95.4	1.3	1.4	95.5	1.5	1.8	97.2	1.2	1.5	97.0
1656.4	994.1	919.8	95.4	6.4	1.5	95.4	5.2	1.9	97.3	6.1	1.6	97.0
1656.6	998.0	922.0	95.1	5.6	1.8	95.3	5.5	1.9	97.2	6.8	1.5	96.9
1656.8	993.2	919.8	95.7	4.3	2.1	95.5	5.0	1.8	97.3	5.9	1.6	97.1
1657.8	984.6	916.5	96.3	3.0	1.7	96.2	3.3	1.4	97.6	4.0	1.2	97.4
1659.0	975.9	913.4	96.7	3.4	1.2	96.6	2.3	1.2	97.8	3.0	1.0	97.5
1659.3	964.9	908.0	97.1	2.0	0.8	97.2	0.6	0.6	97.7	0.5	0.3	97.5
1659.4	969.9	910.7	96.7	2.6	1.2	96.7	1.8	1.1	97.8	2.4	0.8	97.5
1659.9	980.1	916.5	96.4	2.8	1.5	96.3	2.7	1.4	97.7	3.3	1.2	97.5
1660.8	995.9	925.7	95.3	4.6	1.8	95.4	4.6	2.1	97.5	5.3	1.8	97.2
1661.0	986.3	920.9	95.7	3.8	2.1	95.7	3.4	2.0	97.7	3.8	1.7	97.5
1661.0	991.0	923.4	95.2	4.8	2.2	95.4	4.1	2.2	97.6	4.7	2.0	97.3
1664.0	1005.6	934.3	96.4	3.1	1.0	96.4	2.5	1.0	97.4	2.8	0.7	97.1
1664.6	999.4	931.7	95.8	3.3	1.7	95.7	3.8	1.8	97.5	4.5	1.5	97.2
1667.9	993.6	932.5	95.5	4.2	2.3	95.5	3.7	2.2	97.6	4.2	2.0	97.4
1669.1	983.7	928.7	95.4	2.9	2.6	95.4	2.9	2.3	97.8	3.2	2.1	97.6
1670.2	971.9	923.9	95.6	1.4	2.3	95.7	2.2	2.2	97.9	2.5	2.0	97.6
1670.5	998.4	937.9	96.4	2.6	1.5	96.3	3.8	1.2	97.6	5.1	0.9	97.3
1670.8	965.0	921.0	95.8	1.2	2.2	96.0	1.7	1.9	97.9	1.9	1.7	97.6
1672.0	988.5	934.5	95.3	3.4	2.6	95.4	3.2	2.3	97.8	3.6	2.1	97.5
1672.7	1005.4	943.9	97.2	2.2	0.8	97.1	1.5	0.6	97.7	1.7	0.3	97.4
1675.3	991.6	939.8	95.6	2.9	2.4	95.7	3.2	2.1	97.8	3.7	1.8	97.5
1675.7	997.6	943.3	96.2	2.7	1.7	96.2	2.9	1.6	97.8	3.5	1.4	97.6
1678.8	1007.6	951.9	96.5	0.6	1.5	96.6	0.9	1.3	97.9	0.8	1.1	97.7